Electric Power Systems Research 142 (2017) 190–206

Contents lists available at ScienceDirect

Electric Power Systems Research

journal homepage: www.elsevier.com/locate/epsr

Optimal power flow using moth swarm algorithm

Al-Attar Ali Mohamed [a,*], Yahia S. Mohamed [b], Ahmed A.M. El-Gaafary [b], Ashraf M. Hemeida [c]

[a] Electrical Engineering Department, Faculty of Engineering, Aswan University, Egypt
[b] Electrical Engineering Department, Faculty of Engineering, El-Minia University, Egypt
[c] Electrical Engineering Department, Faculty of Energy Engineering, Aswan University, Egypt

ARTICLE INFO

Article history:
Received 3 July 2016
Received in revised form
20 September 2016
Accepted 21 September 2016
Available online 7 October 2016

Keywords:
Optimal power flow
Security constraints
Contingency management
Population diversity crossover
Associative learning mechanism

ABSTRACT

This work presents a novel Moth Swarm Algorithm (MSA), inspired by the orientation of moths towards moonlight to solve constrained Optimal Power Flow (OPF) problem. The associative learning mechanism with immediate memory and population diversity crossover for Lévy-mutation have been proposed to improve exploitation and exploration ability, respectively, in addition to adaptive Gaussian walks and spiral motion. The MSA and four heuristic search algorithms are carried out on the IEEE 30-bus, 57-bus and IEEE 118-bus power systems. These approaches are applied to optimize the control variables such as real power generations, load tap changer ratios, bus voltages and shunt capacitance values under several power system constraints. Fourteen different cases are executed on different curves of fuel cost (e.g., quadratic, valve-loading effects, multi-fuels options), environmental pollution emission, active power loss, voltage profile and voltage stability for contingency and normal conditions, in single and multi objective optimization space. Furthermore, the impacts of the updating mechanism of optimizers on those objective functions are investigated. The effectiveness and superiority of the MSA have been demonstrated in comparison with many recently published OPF solution

1. Introduction

In deregulated power system, OPF is the main tool used to offere the electrical energy at minimum cost with high quality, which is a large-scale, multi-dimensional, non-convex, non-linear, and constrained optimization problem. In this study, the main objectives of OPF problem have been achieved in single/multi-optimization space under different operating conditions.

In recent years, metaheuristic optimization algorithms have been developed for simulating some of chemical, physical and biological phenomena [1]. Several nature-inspired optimization methods have been used to determine the optimized parameters of the power systems for the OPF problem. These algorithms include Adaptive Real Coded Biogeography-Based Optimization (ARCBBO) [2], Grey Wolf Optimizer (GWO) [3], Modified Gaussian Bare-bones Imperialist Competitive algorithm (MGBICA) [4], Artificial Bee Colony (ABC) algorithm[5], Differential Search Algorithm (DSA) [6], Efficient Evolutionary Algorithm (EEA) [7], Particle Swarm Optimization with an Aging Leader and Challengers (ALC-PSO) algorithm [8], Lévy mutation Teaching–Learning-Based Optimization (LTLBO) algorithm [9], Krill Herd Algorithm (KHA) [10], Teaching-Learning-Based Optimization (TLBO) technique [11], Improved Electromagnetism-like Mechanism (IEM) Method [12], Multi-Objective forced initialized Differential Evolution Algorithm (MO-DEA) [13], Fuzzy Harmony Search Algorithm (FHSA) [14], Improved Colliding Bodies Optimization (ICBO) algorithm [15], Hybrid Particle Swarm Optimization and Gravitational Search Algorithm (PSOGSA) [16], Hybrid Modified Particle Swarm Optimization and the Shuffle Frog Leaping algorithms (HMPSO-SFLA) [17], Gravitational Search Algorithm (GSA) [18], Hybrid Shuffle Frog Leaping Algorithm and Simulated Annealing (HSFLA-SA) [19], Gbest guided Artificial Bee Colony (GABC) optimization algorithm [20], and hybrid of Imperialist Competitive Algorithm and Teaching Learning Algorithm (MICA–TLA) [21]. In this paper, the potential and performance capabilities of the proposed MSA are presented in a comparison with all above-mentioned methods.

In the 90's of last century, the most popular nature inspired algorithms have been originated such as Genetic Algorithm (GA), Particle Swarm Optimisation (PSO), Ant Colony Optimisation (ACO) and Differential Evolution (DE). The strategies, operators and coding of those algorithms have been modified to be applied in different science fields [22]. The velocity reflection and Set-On-

* Corresponding author.
E-mail address: engatal@yahoo.com (A.-A.A. Mohamed).

http://dx.doi.org/10.1016/j.epsr.2016.09.025
0378-7796/

Boundary strategies, have been applied on Modified Particle Swarm Optimisation (MPSO) [23], whereas the random uniform distribution has been used to tune mutation and crossover of the Modified Differential Evolution (MDE) [24]. In the proposed algorithm a set of different optimization strategies are hybridized to simulate some of behavioral patterns of the moth swarm.

The development of new algorithms is encouraged by the "No Free Lunch" theorem [25], which states that no single method is best in solving all optimization problems. Therefore, recently there is a dramatic increase in the number of novel algorithms. Those algorithms were proposed inspired by different behavioral rules and key features of the bacterias [26], the cuckoos [27], the frogs [28], etc. The transverse orientation of moths toward artificial lights has been formulated in Moth-Flame Optimization (MFO) algorithm [29], while the pollination process of flowers has been modelled in Flower Pollination Algorithm (FPA) [30]. The two previous algorithms are joined recently to the family of nature-inspired algorithms in the bio-inspired category, and will be tested and compared through this study.

Metaheuristics aim to establish a trade off between the exploitation and exploration, by starting with a high population diversity (high exploration) and decreasing it during the search process. It is noted that, the increase of diversity supports exploration, whereas the decrease of diversity does not necessarily imply a good exploitation or a fast convergence. Therefore, the population diversity is still a stuck problem, and needs a smart treatment [31,32]. In this regard, the hybridization with the mutation originated from GA or DE is one of the most applicable operators to spread the search agents over a wide scope. In the other hand, almost all local search operators (e.g, path finding operator in ACO [33], learning operators in PSO [34] and immune clone and vaccination operators in GA [35]) can be employed for exploiting the solution space in a narrow scope. For that purpose, the DE-mutation and the PSO-learning operators have been included in the MSA method in line with the natural characteristics of the moths.

In the proposed approach, pathfinders in a pure exploration phase use a new adaptive crossover with mutation scaled by Lévy flights for more solutions diversity. Meanwhile, prospectors with logarithmic spiral motion is used to balance exploration–exploitation dilemma. The convergence speed of the MSA is hyperbolic increased by converting the navigation from transverse orientation to celestial navigation adaptively towards the promising areas in the solution space. Hence, onlookers are forced to update its positions with wide (by adaptive Gaussian walks) and narrow (by associative learning mechanism) scope exploitation methods. In addition, most of the control parameters have been adaptively performed to increase the celestial navigation and decrease the transverse orientation during the optimization process.

2. Optimal power flow formulation

Generally, an OPF is a non-convex and nonlinear optimization problem to reduce certain power system objectives subjected to several inequality and equality constraints by determines the best control variables for a given settings of load. The general form of OPF problem can be obtained as follows:

$$\text{Minimize} : f(x,u) \tag{1}$$

$$\text{Subject to} : g(x,u) = 0 \tag{2}$$

$$h(x,u) \le 0 \tag{3}$$

Where, x is vector of system state/dependent variables, u is vector of control/independent variables, $f(x,u)$ is the objective function to be minimized, $g(x,u)$ is the equality constraints and $h(x,u)$ is the inequality constraints. The control and the state variables of the OPF problem are stated as follows:

2.1. State variables

The set of variables, which describe the state of the power system, can be defined as follows:

$$x = \left[P_{G_1}, V_{L_1}, \ldots, V_{L_{NL}}, Q_{G_1}, \ldots, Q_{G_{NG}}, S_{l_1}, \ldots, S_{l_{nl}}\right] \tag{4}$$

Where, P_{G1},Q_G,V_L and S_l are the active power generation at slack bus, reactive power outputs of the generators, the voltage magnitude at load bus and apparent power flow, respectively.*NL*, *NG* and *nl* are the number of load buses (P-Q buses), generators buses (P-V buses) and the transmission lines, respectively.

2.2. Control variables

The set of parameters, which can be control the power flow equations, are represented in terms of the decision vector as follows:

$$u = \left[P_{G_2}, \ldots, P_{G_{NG}}, V_{G_1}, \ldots, V_{G_{NG}}, T_1, \ldots, T_{NT}, Q_{C_1}, \ldots, Q_{C_{NC}}\right] \tag{5}$$

Where, P_G is the generator active power, V_G is the generators voltage magnitude, T is the transformer tap, Q_c is the reactive power of shunt VAR compensators, *NT* and *NC* are the number of regulating transformers and shunt VAR compensators units, respectively.

2.3. Constraints

The problem of OPF has to fulfill both inequality and equality constraints. The power balance constraints are considered as equality constraint. The operating limits of power system components are considered as inequality constraints.

2.3.1. Equality constraints

These constraints represent the typical load flow equations using the balance of the active and reactive power, as follows:

$$P_{Gi} - P_{Di} - V_i \sum_{j=1}^{nb} V_j [G_{ij} cos(\delta_i - \delta_j) + B_{ij} sin(\delta_i - \delta_j)] = 0 \, \forall \, i \varepsilon nb \tag{6}$$

$$Q_{Gi} - Q_{Di} - V_i \sum_{j=1}^{nb} V_j [G_{ij} sin(\delta_i - \delta_j) - B_{ij} cos(\delta_i - \delta_j)] = 0 \, \forall \, i \varepsilon nb \tag{7}$$

Where, *nb* is the total number of buses, Q_G is the generator reactive power, P_D is the active load demand, Q_D is the reactive load demand, G_{ij} and B_{ij} are the transfer conductance and susceptance between bus i and bus j, respectively. These constraints are strictly enforced during the load flow procedure, which guarantees that the searched optimal solution is feasible.

2.3.2. Inequality constraints

These constraints represent the power system operating limits as follows:

Generation constraints: For stable operation, the voltages, real power, and reactive power of the generators are restricted by the lower and upper limits as follows:

$$P_{Gi}^{\min} \le P_{Gi} \le P_{Gi}^{\max} \, \forall \, i \varepsilon NG \tag{8}$$

$$Q_{Gi}^{\min} \le Q_{Gi} \le Q_{Gi}^{\max} \, \forall \, i \varepsilon NG \tag{9}$$

$$V_{Gi}^{\min} \le V_{Gi} \le V_{Gi}^{\max} \, \forall \, i \varepsilon NG \tag{10}$$

Transformer constraints: The tap settings of the transformers must be restricted by their upper and lower limits as follows:

$$T_i^{\min} \le T_i \le T_i^{\max} \ \forall i \varepsilon NT \tag{11}$$

Security constraints: The constraints of load buses voltage magnitudes and transmission line loadings ought to be restricted within their limits as follows:

$$V_{Bi}^{\min} \le V_{Bi} \le V_{Bi}^{\max} \ \forall i \varepsilon NL \tag{12}$$

$$S_{Li} \le S_{Li}^{\max} \ \forall i \varepsilon \mathrm{nl} \tag{13}$$

Shunt VAR compensator constraints: The shunt VAR compensators are restricted by their limits as follows:

$$Q_{ci}^{\min} \le Q_{ci} \le Q_{ci}^{\max} \forall i \varepsilon NC \tag{14}$$

2.3.3. Constraints handling

The inequality constraints of dependent variables contain real power generation output at slack bus, load bus voltage magnitude, reactive power generation output and line loading are incorporated into the extended objective function to keep the dependent variables within their permissible limits and to decline any infeasible solution. The penalty function can be defined by a quadratic terms as follows [36]:

$$Penalty = K_P(P_{G1} - P_{G1}^{Lim})^2 + K_Q \sum_{i=1}^{NG} (Q_{Gi} - Q_{Gi}^{Lim})^2 + K_V \sum_{i=1}^{NL} (V_{Bi} - V_{Bi}^{Lim})^2 + K_S \sum_{i=1}^{nl} (S_{Li} - S_{Li}^{Lim})^2 \tag{15}$$

Where K_P, K_Q, K_V and K_S are the penalty factors having large positive value, which is specified as 100 except the load voltage (K_V) is set to 100,000 [13]. x^{Lim} is the violated limit value of the dependent variable x given as:

$$x^{Lim} = \begin{cases} x^{max} \text{ if } x > x^{max} \\ x^{min} \text{ if } x < x^{min} \end{cases} \tag{16}$$

3. Proposed moth-swarm algorithm

3.1. Source of inspiration

Lepidoptera (butterflies and moths) is the second largest order in the insect class, which represents over 53% of all species on earth. Moths and other nocturnal insects try to hide from predators during daylight, and at night they use the celestial navigation technique to orient in the dark and exploit the food sources. The moths fly in a straight line over a long distance by steer their locomotion in a constant angle relative to celestial far-distant point light e.g., moonlight, which is also known as the light compass reaction. Nevertheless, such orientation suffers from a transverse direction motion due to futile spiral tracks around nearby artificial light source. [37,38].

3.2. Basic concepts

In the proposed MSA, the possible solution of optimization problem is represented by position of light source, and the fitness/quality of this solution is considered as luminescence intensity of the light source. These assumptions have been used to approximate the characteristics of the proposed algorithm. In addition, the proposed moth swarm is considered to consist of three groups of moths, which may be defined as follows:

Pathfinders: A small group of moths (n_p) that has ability to discover the new areas over the optimization space with principle of First In-Last Out. The main task of this type is to discriminate the best positions as a light sources to guide the movement of the main swarm (i.e, light the way).

Prospectors: A group of moths that tends to wander into a random spiral path within the neighborhood of the light sources, which have been marked by the pathfinders.

Onlookers: A group of moths that drift directly toward the best global solution (moonlight), which has been obtained by prospectors.

3.3. Mathematical explanation

At any iteration, each moth x_i is incorporated into the optimization problem to find the luminescence intensity of its corresponding light source $f(x_i)$. The best fitnesses in the swarm are considered as the positions of the pathfinders, and guidance for the next update iteration. Hence, the second and third best groups take the name of the prospectors and onlookers, respectively. The proposed optimization algorithm has been executed through the following phases:

3.3.1. Initialization

At the start of the flight, for d-dimensional problem and n number of population, the positions of the seach agent moths (initial candidate solutions) are randomly created as follows:

$$x_{ij} = rand[0,1] \cdot \left(x_j^{max} - x_j^{min}\right) + x_j^{min} \quad \forall i \in \{1,2,\ldots,n\}, j \in \{1,2,\ldots,d\} \tag{17}$$

Where, x_j^{max} and x_j^{min} are the upper and lower limits, respectively.

After initialization, the type of each moth in the swarm is selected based on its calculated fitness. Therefore, the best moths are chosen to be the light sources (pathfinders), and the next best and worse groups of moths are dealt as a prospectors and onlookers, respectively.

3.3.2. Reconnaissance phase

In the proposed MSA algorithm, the swarm quality for exploration may be decreased during the optimization process. The moths can be concentrated in the regions may seem it is a good, causing a stagnation situation. To obviate the precocious convergence and improve the diversity of solutions, a part of the swarm is obligated to discover the less-crowded area. The pathfinder moths, which play this role, are updated its position by interacting with each others (crossover operations) with an ability to fly for long distance (lévy-mutation) using the proposed adaptive-crossover with lévy-mutation, which is described in the next five steps:

3.3.2.1. Proposed diversity index for crossover points. A new strategy for the solutions diversity is proposed to select the crossover points. First, for t iteration, the normalized dispersal degree σ_j^t of the individuals in the jth dimension is measured as follows:

$$\sigma_j^t = \frac{\sqrt{\frac{1}{n_p}\sum_{i=1}^{n_p}\left(x_{ij}^t - \overline{x_j^t}\right)^2}}{\overline{x_j^t}} \tag{18}$$

Where, $\overline{x_j^t} = \frac{1}{n_p}\sum_{i=1}^{n_p} x_{ij}^t$, and n_p is the number of pathfinders moths. Then the variation coefficient μ^t, which is a measure for relative dispersion, may be formulated as follows:

$$\mu^t = \frac{1}{d}\sum_{j=1}^{d} \sigma_j^t \tag{19}$$

Any component of pathfinder moth suffers from a low degree of dispersal will be accepted in the crossover points group c_p, as described in the next requirement.

$$j \in c_p \text{ if } \sigma_j^t \le \mu^t \tag{20}$$

It can be seen that, the group of crossover points is dynamically changed with the progress of the proposed strategy.

3.3.2.2. Lévy flights. Lévy flights/motions are random processes based on α-stable distribution with ability to travel over large scale distances using different size of steps. Lévy α-stable distribution strongly linked with heavy-tailed probability density function (PDF), fractal statistics, and anomalous diffusion. The PDF of the individual jumps $\lambda(q) \sim |q|^{-1-\alpha}$ decaying at large generated variableq [39]. The stability/tail index $\alpha \in [0,2]$ or so called the characteristic exponent describes the rate at which the tails of the distribution taper off (decay), which is slower for larger values of the tail index [40]. There are a few special cases have a close form for the density of the general Lévy distribution, can be defined as:

- Gaussian or normal distribution, $q \sim N\left(\mu, \sigma_G^2\right)$ if density is:

$$f(q) = \frac{1}{\sqrt{2\pi}\sigma_G} exp\left(-\frac{(q-\mu)^2}{2\sigma_G^2}\right) -\infty < q < \infty \tag{21}$$

- Cauchy distribution, $q \sim cauchy(\sigma, \mu)$ if density is:

$$f(q) = \frac{1}{\pi\left(\sigma^2 + (q-\mu)^2\right)} -\infty < q < \infty \tag{22}$$

- A simple version of Lévy distribution, $q \sim Levy(\sigma, \mu)$ if density is:

$$f(q) = \sqrt{\frac{\gamma}{2\pi}} \frac{1}{(q-\mu)^{3/2}} exp\left(-\frac{\sigma}{2(q-\mu)}\right) 0 < \mu < q < \infty \tag{23}$$

The Lévy distribution achieves the heavier tail than the other cases. Mantegna's algorithm [41] is used to emulate the α-stable distribution by generating random samples L_i that have the same behaviour of the Lévy-flights, as follows:

$$L_i \sim step \oplus Levy(\alpha) \sim 0.01 \frac{u}{|y|^{1/\alpha}} \tag{24}$$

Where, *step* is the scaling size related to the scales of the interest problem, $\oplus$ is the entrywise multiplications, $u = N\left(0, {\sigma_u}^2\right)$ and $y = N\left(0, {\sigma_y}^2\right)$ are two normal stochastic distributions with $\sigma_u = \left[\frac{\Gamma(1+\alpha)\sin\pi\alpha/2}{\Gamma\left((1+\alpha)/2\alpha 2^{(\alpha-1)/2}\right)}\right]^{1/\alpha}$ and $\sigma_y = 1$.

3.3.2.3. Difference vectors Lévy-mutation. For $n_c \in c_p$ crossover operations points, the proposed algorithm creates the sub-trial vector $\vec{v_p} = \left[v_{p1}, v_{p2}, \ldots, v_{pn_c}\right]$ by perturbing the selected components of the host vector $\vec{x_p} = \left[x_{p1}, x_{p2}, \ldots, x_{pn_c}\right]$, with related components in the donor vectors (e.g., $\vec{x_{r^1}} = \left[x_{r^1 1}, x_{r^1 2}, \ldots, x_{r^1 n_c}\right]$). The Mutation strategy may be used for synthesis such a sub-trail vector, as follows:

$$\vec{v_p^t} = +L_{p1}^t \cdot \left(\vec{x_{r2}^t}, -, \vec{x_{r3}^t}\right) + L_{p2}^t \cdot \left(\vec{x_{r4}^t}, -, \vec{x_{r5}^t}\right)$$
$$\forall r^1 \ne r^2 \ne r^3 \ne r^4 \ne r^5 \ne p \in \{1, 2, \ldots, n_p\} \vec{x_{r1}^t} \tag{25}$$

Where, L_{p1} and L_{p2} are two independent identical variables used as the mutation scaling factor and generated by a heavy tail Lévy-flights using $\left(L_p \sim \text{random}(n_c) \oplus Levy(\alpha)\right)$. The set of mutually indices $(r^1, r^2, r^3, r^4, r^5, p)$ are exclusively selected from the pathfinder solutions.

3.3.2.4. Proposed adaptive crossover operation based on population diversity. In order to achieve the completed trail solution, each pathfinder solution (host vector) updates its position through the crossover operations by incorporated the mutated variables of the sub-trail vector (low degree of dispersal) into the corresponding variables of host vector. The completed trail/mixed solution V_{pj}, may be described as:

$$V_{pj}^t = \begin{cases} v_{pj}^t \text{ if } j \in c_p \\ x_{pj}^t \text{ if } j \notin c_p \end{cases} \tag{26}$$

It must be noted that, the variation coefficient μ^t is not used here as a validation index, but it is used to control the crossover rate. This operation may be extended to use other statistical metrics for controlling the characteristics behaviour of any metaheuristic optimization algorithms in the future.

3.3.2.5. Selection strategy. After the previous procedure was completed, the fitness value of the completed trail solution is calculated and compared with its corresponding host solution. The fitter solutions are selected to survive for the next generation, which may be outlined for minimization problems as follows:

$$\vec{x_p^{t+1}} = \begin{cases} \vec{x_p^t} \text{ if } f\left(\vec{V_p^t}\right) \ge f\left(\vec{x_p^t}\right) \\ \vec{v_p^t} \text{ if } f\left(\vec{V_p^t}\right) < f\left(\vec{x_p^t}\right) \end{cases} \tag{27}$$

The probability value P_p is estimated proportional to luminescence intensity fit_p, as follows:

$$P_p = \frac{fit_p}{\sum_{p=1}^{n_p} fit_p} \tag{28}$$

The luminescence intensity is calculated from the objective function value f_p for minimization problems as:

$$fit_p = \begin{cases} \frac{1}{1+f_p} \text{ for } f_p \ge 0 \\ 1 + |f_p| \text{ for } f_p < 0 \end{cases} \tag{29}$$

3.3.3. Transverse orientation

Conical logarithmic spirals is frequently occurring in nature and broadly studied by scientists [42]. A set of trajectories that circumscribe the surface of a cone have been described for insect flight path towards a source of light by holding the conical apex at a fixed angle [43]. The idea has been reduced to two dimensions, resulting in planar spiral in MFO [29] algorithm. The group of moths that have the next best luminescence intensities are set to be the prospectors. Over the course of iterations T the number of prospectors n_f is proposed to decrease as follows:

$$n_f = round\left(\left(n - n_p\right) \times \left(1 - \frac{t}{T}\right)\right) \tag{30}$$

Each prospector x_i is proposed to update its position according to the spiral flight path shown in Fig. 1(a), which may be mathematically expressed as follows:

$$x_i^{t+1} = |x_i^t - x_p^t| \cdot e^{\theta} \cdot \cos 2\pi\theta + x_p^t$$
$$\forall p \in \left\{1, 2, \ldots, n_p\right\}; i \in \left\{n_p + 1, n_p + 2, \ldots, n_f\right\} \tag{31}$$

Where, $\theta \in [r, 1]$ is a random number to define the spiral shape and $r = -1 - t/T$.

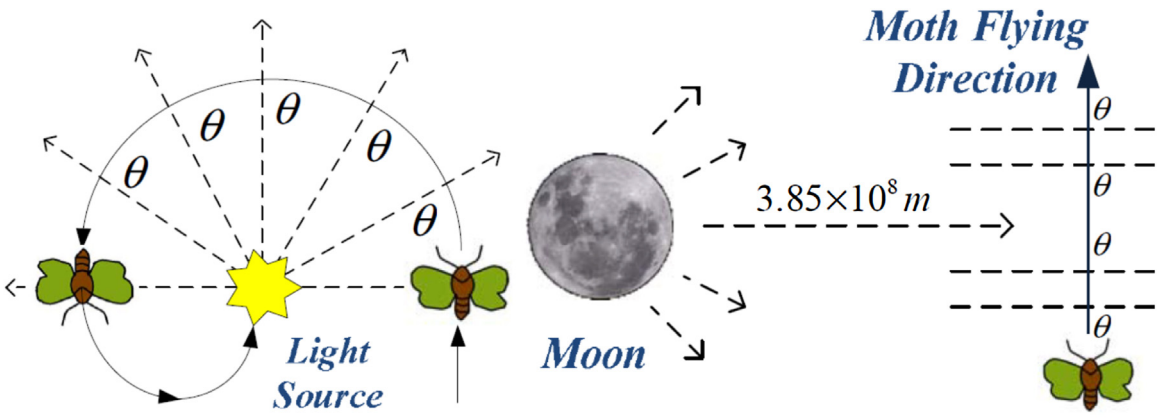

(a) Moths fly in a spiral path into nearby light source.

(b) Moths flying in a fixed angle relative to moonlight.

Fig. 1. Orientation behaviour of moth swarm.

In Eq. (31) we use the logarithmic flight path in MFO algorithm. However, two modification have been applied on this planar motion. First, it was modified to deal with each variable/moth as an integrated unit for reducing the computational cost. Secondly, the light source x_p (flame) was chosen on the basis of the probability function P_p using Eq. (28) to improve the ability for exploitation.

In the MSA model, the type of each moth is dynamically changed. Hence, any prospector moth finds a solution more luminescence than the existing light sources, promotes to become pathfinder moth. Meaning that, the new lighting sources and moonlight will be present at the end of this stage.

3.3.4. Celestial navigation

During the optimization process, the decreasing in the number of prospectors increases the number of onlookers ($n_o = n - n_f - n_p$), which may lead to a rapid increase in the speed of convergence rate of the proposed algorithm towards global solution. The moths that have the lowest luminescent sources in the swarm are considered onlookers moths. These moths aims to travel directly to the most shining solution (the moon) Fig. 1(b). In this phase, the MSA is designed to force the onlookers to search more effectively by zooming in on the hot spots of the prospector. The onlookers are splited in the following two parts.

3.3.4.1. Gaussian walks. In this phase we want to focus on promising areas in the search space. Gaussian stochastic distribution can be used to play this role, due to its ability to limit distributions of random samples, and consequently limits the variation in the next population positions. The first part, with size equal to $n_G = round\left(n_o/2\right)$, walks according to Gaussian distributions using Eq. (21). The new onlooker moth in this sub-group x_i^{t+1} moves with series steps of Gaussian walks, which may be described as follows:

$$x_i^{t+1} = x_i^t + \varepsilon_1 + \left[\varepsilon_2 \times best_g^t - \varepsilon_3 \times x_i^t\right]; \forall i \in \left\{1, 2, \ldots, n_G\right\} \quad (32)$$

$$\varepsilon_1 \sim random\left(size\left(d\right)\right) \oplus N\left(best_g^t, \frac{\log t}{t} \times \left(x_i^t - best_g^t\right)\right) \quad (33)$$

Where, ε_1 is a random samples drawn from Gaussian stochastic distribution scaled to the size of this group, $best_g$ is the global best solution obtained by the transverse orientation phase (both prospectors and pathfinders), ε_2 and ε_3 are random numbers distributed uniformly within the interval [0,1].

3.3.4.2. Associative learning mechanism with immediate memory. A kind of memory exists in many optimization algorithms to transfer information from generation to next generation. However in a real world, the moths fall into the fire because they do not have an evolutionary memory. The behaviour of moths is strongly influenced by the associative learning and the short-term memory (1–3 s) [44,45]. The associative learning capabilities play a major role in communication between moths [46,47]. Therefore, the second part of onlookers moths, with size equal to $n_A = n_o - n_G$, are employed to drift towards the moon light according to the associative learning operators with an immediate memory to mimic the actual behaviour of moths in nature. The immediate memory is initialized from the continuous uniform Gaussian distribution on the interval from $x_i^t - x_i^{min}$ to $x_i^{max} - x_i^t$. The updating equation of this type may be completed in form:

$$x_i^{t+1} = x_i^t + 0.001 \cdot G\left[x_i^t - x_i^{min}, x_i^{max} - x_i^t\right] + \left(1 - g/G\right) \cdot r_1 \cdot \left(best_p^t - x_i^t\right) + 2g/G \cdot r_2 \cdot \left(best_g^t - x_i^t\right) \quad (34)$$

Where, $i \in \left\{1, 2, \ldots, n_A\right\}$, $2g/G$ is the social factor, $1 - g/G$ is the cognitive factor, and r_1 and r_2 are random number within the interval [0,1]. Similar to transverse orientation phase, $best_p$ is a light source randomly chosen from the new pathfinders group based on the probability value of its corresponding solution.

As mentioned earlier, at each iteration end, the fitness values of the whole swarm become available to refine the type of each moth for the next iteration. The flowchart of the proposed MSA is shown in Fig. 2. The source codes of the MSA are available at:

https://www.mathworks.com/matlabcentral/fileexchange/57822 –moth-swarm-algorithm–msa-

3.4. Implementation of MSA to solve OPF problem

In this section, we discussed the detail procedure to apply MSA based approach for solving OPF problem. The control variables of OPF problem constitute the individual position of moth that represent a complete candidate solution set of the OPF problem. According to Eq. (5), the size of control vector can be obtained as follows:

$$d = 2NG + NT + NC - 1 \quad (35)$$

The position of the ith seach agent moth, consisting of d number of control variables, can be defined as follows:

$$x_i = \begin{pmatrix} x_{i1} & x_{i2} & \ldots & x_{id} \end{pmatrix} \quad (36)$$

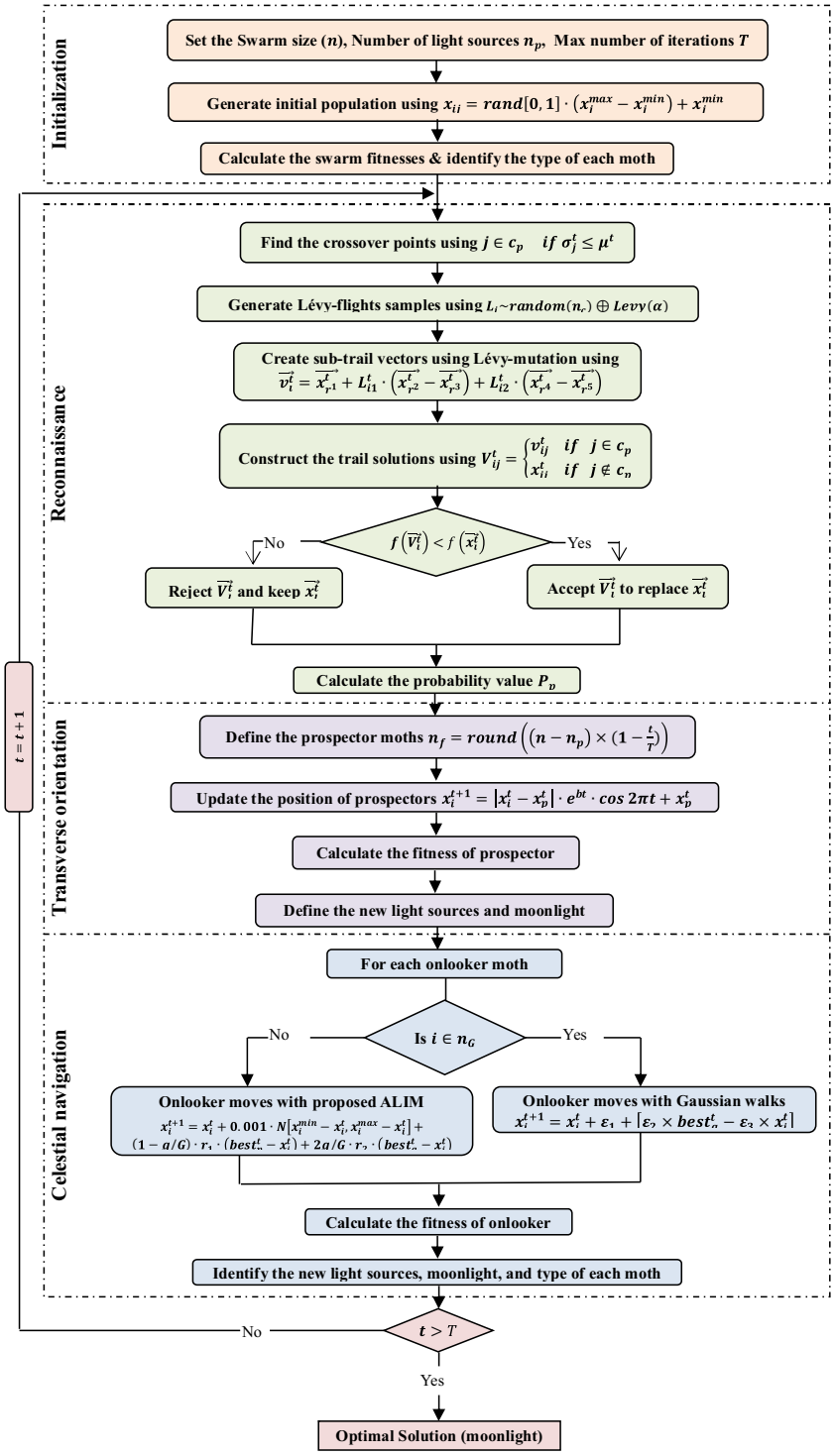

Fig. 2. The flowchart of the proposed MSA.

In a swarm with n moths, the seach agents together form the swarm matrix X as,

$$X = \begin{bmatrix} x_{11} & x_{12} & \dots & x_{1d} \\ x_{21} & x_{22} & \cdots & x_{2d} \\ \vdots & \vdots & \vdots & \vdots \\ x_{n1} & x_{n2} & \dots & x_{nd} \end{bmatrix} \quad (37)$$

Different steps to solve the OPF problem using MSA are illustrated in the following proceedings:

1 The elements of the swarm matrix are randomly initialized between maximum and minimum values of the control variables according to (17).
2 The type of each moth is identified based on its fitness.

3 New pathfinders are generated with the help of (20) and (24)-(27), the prospectors are updated according to (31) and the onlookers are moved according to thier type using (32)-(34).
4 The fitness value for each new member of swarm is calculated.
5 Steps 2–4 are repeated until the termination criterion is satisfied.
6 The global best solution (moonlight) is availabled.

4. Optimal power flow simulation results based on MSA

The IEEE 30-bus, IEEE 57-bus and the IEEE 118-bus systems are used to test the simulation effect of the MSA paradigm for solving OPF problem. In addition, 14 different case studies are investigated, which are summarized in Table 1. The maximum number of iterations is set to 100 for the first two systems, and set to 500 for IEEE 118-bus system. The main characteristics of these systems are summarized in Table 2. The MSA is tested and compared with four algorithms, namely MPSO [23], MDE [24], MFO [29], and FPA [30] using the setting of the control-parameters given in Table 3. All programs were implemented in MATLAB 7.7 (R2008b) on a PC with an Intel® Core 4 CPU 3.0 GHz 2.0 GB RAM.

4.1. IEEE 30-bus system

The IEEE 30-bus system has been used to illustrate the effectiveness of the proposed algorithm. The line data and the bus data are given in [48]. The system active and reactive power demands are 2.834 p.u and 1.262 p.u, respectively, at 100 MVA base. Different cases are considered to investigate the basic and complex objective functions. A swarm of 50 moths with seven pathfinders of MSA has been implemented to solve the OPF problem for several cases with different objective functions. The control variables limits are included in Table 4, as given in [49]. The control parameters obtained by the MSA and the values of related objective functions are presented in the same table. In addition, the MPSO, MDE, MFO and PFA algorithms are implemented to solve all cases under the same conditions, i.e., system data, constraints, control variables limits and population size.

4.1.1. Single objective optimal power flow

The first five cases are considered to solve the single objective OPF problems. The best solutions of the algorithms under study are compared with the results of MSA, as summarized in Table 5. In addition, a comparative study with other heuristic techniques reported in the literature is given in Table 6.

Case 1: minimization of basic fuel cost

The objective function considering minimization the total fuel cost of power generation is taken as the first single objective function, and it can be formulated by a quadratic curve as follows:

$$f = \left(\sum_{i=1}^{NG} a_i P_{Gi}^2 + b_i P_{Gi} + c_i\right) + \text{Penalty}(\$/h) \tag{38}$$

Where, and a_i, b_i and c_i are the cost coefficients of ith generator. For this case, the MSA and MPSO produce a better solutions compared to the MDE and MFO methods, whereas the best fuel cost value obtained by FPA is much more than the rest of algorithms. In the field of convergence characteristics, the MSA and MPSO have smooth curves with a speedy convergence rate more than the other algorithms, as shown in Fig. 3(a).

Case 2: minimization of piecewise quadratic fuel cost functions

From the operation conditions of power system, the thermal generators may have several fuel sources like oil, natural gas, and coal. Thus, the mathematical formulation for the fuel cost curve of these generators (units 1 and 2) can be considered as a set of constraints as follows:

$$F_{mf\_cost} = \begin{cases} a_{i1}P_{Gi}^2 + b_{i1}P_{Gi} + c_{i1} \;\; P_{Gi}^{min} \le P_{Gi} \le P_{Gi1} \\ a_{i2}P_{Gi}^2 + b_{i2}P_{Gi} + c_{i2} \;\; P_{Gi1} \le P_{Gi} \le P_{Gi2} \\ \vdots \\ a_{ik}P_{Gi}^2 + b_{ik}P_{Gi} + c_{ik} \;\; P_{Gik-1} \le P_{Gi} \le P_{Gi}^{max} \end{cases} \tag{39}$$

Where, a_{i2}, b_{ik} and c_{ik} indicate cost coefficients of the ith generator for k type of fuel. Clearly, the cost coefficients of the remaining single fuel source units remain intact and have the same values as case 1. Thus, the objective function used to model the fuel cost characteristics can be expressed as follows:

$$f = \left(\sum_{i=1}^{2} a_{ik}P_{Gi}^2 + b_{ik}P_{Gi} + c_{ik}\right) + \left(\sum_{i=3}^{NG} a_i P_{Gi}^2 + b_i P_{Gi} + c_i\right) + Penalty(\$/h) \tag{40}$$

It must be mentioned here that, the choice of the optimization method is closely related to the type of objective function as well as the constraints [50]. Therefore, the Set On Boundary and Velocity Mirror strategies of MPSO may have a good ability to deal with the complicated boundaries in this type of problems. Thus, the MPSO has the best solution to minimize of fuel cost in this case. Meanwhile, the MSA has the second best final solution with more convergence rate as depicted in Fig. 3(b). On the other hand, the MDE, MFO, and FPA still suffer from excessively slow convergence.

Table 7 uses this objective function to assess the convergence speed of the proposed algorithm. The MFO algorithm required less computation time than the other techniques. This is because MFO uses a single updating equation even though it applies to each component of variables.

Although, the MSA contains a number of strategies, but each of them apply to a certain group of the population. Except pathfinders group, all moths are dealing with each variable as an integrated unit. In addition, no longer need to store the positions, velocities, and personal best solution for each onlooker moth, as in the basic PSO. These properties have made the MSA gives acceptable results.

The MPSO has a higher cpu-time than the other methods, which may be attributed for the application of the two modifications on all particles. It is important to point out that, the MPSO and MSA, in general, have the highest convergence speed and therefore the quickest answer to the problem at hand.

In order to evaluate the robustness of the proposed paradigm, a comparison in terms of best, average and worse fuel cost is given in Table 8. This table is evident that, the frequency of getting best fuel cost value by MSA method for 30 trial run is better than other algorithms.

Case 3: minimization of quadratic fuel cost with valve-point loadings

In this case, the valve-loading effects are modelled as an absolute sinusoidal function added to the cost characteristics of the considered units 1 and 2, as follows:

$$F_{vl\_cost} = a_i P_{Gi}^2 + b_i P_{Gi} + c_i + |d_i sin\left(e_i\left(P_{Gi}^{min} - P_{Gi}\right)\right)| \;\; \forall i = 1, 2 \tag{41}$$

where a_i, b_i, c_i, d_i and e_i are the cost coefficients of the ith unit. The cost coefficients of other units have the same values as case 1.

The fuel cost objective function can be expressed as follows:

$$f = \left(\sum_{i=1}^{2} a_i P_{Gi}^2 + b_i P_{Gi} + c_i + |d_i sin\left(e_i\left(P_{Gi}^{min} - P_{Gi}\right)\right)|\right) + \left(\sum_{i=3}^{NG} a_i P_{Gi}^2 + b_i P_{Gi} + c_i\right) + Penalty \tag{42}$$

Table 1
Different case studies investigated in this paper.

Name	Objective function to be minimized	Constraints	Test system
Case 1	quadratic fuel cost	Equality and non-equality	IEEE 30
Case 2	piecewise quadratic fuel cost	Equality, non-equality and prohibited zones	
Case 3	quadratic fuel cost curve with valve-point loading	Equality and non-equality	
Case 4	emission cost	Equality and non-equality	
Case 5	active power loss	Equality and non-equality	
Case 6	quadratic fuel cost considering active power loss	Equality and non-equality	
Case 7	quadratic fuel cost considering voltage profile	Equality and non-equality	
Case 8	quadratic fuel cost considering voltage stability	Equality and non-equality	
Case 9	quadratic fuel cost considering voltage stability during contingency	Equality and non-equality for N−1.	
Case 10	quadratic fuel cost considering power loss, voltage profile and voltage stability	Equality and non-equality	
Case 11	quadratic fuel cost	Equality and non-equality	IEEE 57
Case 12	quadratic fuel cost considering voltage profile	Equality and non-equality	
Case 13	quadratic fuel cost considering voltage stability	Equality and non-equality	
Case 14	quadratic fuel cost	Equality and non-equality	IEEE 118

Table 2
The main characteristics of the studied systems.

IEEE 30			IEEE 57		IEEE 118	
characteristics	*Value*	*Details*	*Value*	*Details*	*Value*	*Details*
Buses	30	[48]	57	[52]	118	[52]
Branches	41	[48]	80	[52]	186	[52]
Generators	6	Buses: **1**, 2, 5, 8, 11 and 13	7	Buses: **1**, 2, 3, 6, 8, 9 and 12.	54	Buses: **1**, 4, 6, 8, 10, 12, 15, 18, 19, 24, 25, 26, 27, 31, 32, 34, 36, 40, 42, 46, 49, 54, 55, 56, 59, 61, 62, 65, 66, 69, 70, 72, 73, 74, 76, 77, 80, 85, 87, 89, 90, 91, 92, 99, 100, 103, 104, 105, 107, 110, 111, 112, 113 and 116.
Load voltage limits	24	[0.95−1.05]	50	[0.94−1.06]		[0.94–1.06]
Shunts VAR compensation	9	Buses: 10, 12, 15, 17, 20, 21, 23, 24 and 29.	3	Buses: 18, 25 and 53.	14	Buses: 5, 34, 37, 44, 45, 46, 48, 74, 79, 82, 83, 105, 107 and 110
transformers with off-nominal tap ratio	4	Branches: 11, 12, 15 and 36.	17	Branches: 19, 20, 31, 35, 36, 37, 41, 46, 54, 58, 59, 65, 66, 71, 73, 76 and 80.	9	Branches: 8, 32, 36, 51, 93, 95, 102, 107 and 127.
Control variables	24	–	33	–	130	–

Table 3
control-parameters values for the differnt algorithms.

MPSO	**MDE**	**MFO**	**FPA**
Personal Coefficient: c1 = 2 Global Coefficient: c2 = 2 Inertia Damping Ratio: Wdamp = 0.99. Inertia Weight: w = 1	Strategy: best/1/bin Mutation factor: MF = 0.5 Crossover rate: CR = [0.2, 0.8]	Shape constant: b = 1	Probability switch: P = 0.8 standard gamma function: λ=1.5

The updating mechanism of MFO is mainly depends on a logarithmic spiral path. This mechanism has somewhat the same form of the current objective function, and thus may be more able to deal with it. Thus, a smooth convergence characteristic of MFO has been depicted in Fig. 3(c). The final solution of MSA is very close to the results of MFO. On the other hand, MPSO suffer from a premature convergence, caused by particles stagnating around local optima, when handling such nonlinear functions.

Case 4: minimization of emission cost

In the present case, the objective is to minimize the emission level of the two important pollution gases, i.e. NOX and SOX, which can be written in the following form:

$$f = \sum_{i=1}^{NG} \gamma_i P_{Gi}^2 + \beta_i P_{Gi} + \alpha_i + \zeta_i e^{(\lambda_i P_{Gi})} + Penalty\left(ton/h\right) \quad (43)$$

Where γ_i, β_i, α_i,ζ_i and λ_i are the emission coefficients of ith unit.

The usefulness of the algorithms depends crucially on the form of objective function. The variations of emission cost over the iterations are sketched in Fig. 3(d). The MSA achieved the best final solution, while the FPA with Lévy-flights provided a superior performance than the rest of algorithms. Non-existence of the sinus in this function may be a reason for a slight decline in the efficiency of MFO algorithm. In addition, as in previous case, the MPSO obtained the worst performance.

Case 5: minimization of power loss

This case aimed to decrease the active power loss for each transmission line by minimization of the following objective function:

$$f = \sum_{i=1}^{nl} \sum_{j \neq i}^{nl} G_{ij} V_i^2 + V_j^2 - 2V_i V_j cos\left(\delta_i - \delta_j\right) + Penalty\,(MW) \quad (44)$$

The convergence characteristics of the power loss are shown in Fig. 3(e). The performances of algorithms in the current case are similar to case 1. Part of the reason may be that the objective function forms of these cases have some similarities. Thus, the MSA achieves the best performance, while FPA obtains the worst one.

4.1.2. Multi-objective optimal power flow

Generally, solving multi-objective problems is used to optimize simultaneously different independent objective functions. Five dif-

Table 4
Optimal solutions obtained by MSA for IEEE 30 system.

Control variables	Min	Max	Case 1	Case 2	Case 3	Case 4	Case 5	Case 6	Case 7	Case 8	Case 9	Case 10
P_{G2} (MW)	20	80	48.7326	54.9952	51.9685	67.6392	80	55.0797	48.7218	47.0661	47.9242	52.5624
P_{G5} (MW)	15	50	21.4572	24.0916	15.0004	50	50	38.2097	21.8452	21.5451	21.3747	31.5466
P_{G8} (MW)	10	35	21.0638	35	10	35	35	34.9995	22.2104	21.0438	23.9205	34.9913
P_{G11} (MW)	10	30	11.9657	19.5076	10	30	30	29.9947	12.1357	14.7626	12.6431	26.5086
P_{G13} (MW)	12	40	12.0021	16.6129	12	40	40	26.8439	12.0022	12.317	12	21.4272
V_1 (PU)	0.95	1.10	1.0848	1.07517	1.03356	1.06282	1.06187	1.06944	1.05052	1.07742	1.08773	1.07067
V_2 (PU)	0.95	1.10	1.0653	1.05679	1.01127	1.05642	1.05766	1.05856	1.0313	1.0616	1.07089	1.05748
V_5 (PU)	0.95	1.10	1.03386	1.02613	0.971351	1.03743	1.03811	1.0346	1.01057	1.0331	1.03405	1.03024
V_8 (PU)	0.95	1.10	1.03823	1.03535	1.03439	1.04358	1.04422	1.04288	1.00766	1.04836	1.02777	1.03906
V_{11} (PU)	0.95	1.10	1.0927	1.06816	1.09929	1.07504	1.07203	1.08952	1.02101	1.0999	1.09126	1.00917
V_{13} (PU)	0.95	1.10	1.04533	1.07765	1.09992	1.05341	1.05906	1.05493	0.992125	1.05084	1.06292	1.03987
T_{11} (PU)	0.90	1.10	1.04907	0.992267	1.1	1.09961	1.09074	1.024	1.03943	1.04275	1.02531	1.0558
T_{12} (PU)	0.90	1.10	0.938762	0.958006	1.0532	0.900732	0.900009	0.962817	0.900965	0.90553	0.936761	0.939783
T_{15} (PU)	0.90	1.10	0.970177	1.02422	1.06973	0.996876	0.997851	0.98958	0.953765	0.974468	1.01206	1.06393
T_{36} (PU)	0.90	1.10	0.97498	0.968961	1.06513	0.976927	0.976541	0.976004	0.956971	0.971978	0.959546	1.00596
Q_{c10} (MVAR)	0.00	5	2.37123	2.79614	4.98433	4.99654	4.99998	1.98213	5	3.38991	1.83754	2.22721
Q_{c12} (MVAR)	0.00	5	2.57918	3.48842	4.99678	4.99781	0.767227	1.68599	2.2444	1.83146	5	1.99685
Q_{c15} (MVAR)	0.00	5	4.20734	2.97278	4.99345	3.33964	4.22968	4.18104	4.75979	2.98534	5	4.45733
Q_{c17} (MVAR)	0.00	5	5	1.73784	4.99414	4.99897	5	5	0.271973	1.09045	5	2.51507
Q_{c20} (MVAR)	0.00	5	3.68771	3.36806	4.65486	4.9998	3.96706	3.62953	4.99208	0.673286	2.83784	3.93636
Q_{c21} (MVAR)	0.00	5	4.95747	4.2466	4.99686	4.99845	5	4.95832	4.9143	3.74157	5	4.99047
Q_{c23} (MVAR)	0.00	5	3.08148	3.90944	4.99969	2.95234	3.01344	2.88178	4.82359	2.45557	5	4.32656
Q_{c24} (MVAR)	0.00	5	4.98767	2.36029	4.99499	4.99802	4.99999	4.99866	4.93992	2.34699	5	4.96993
Q_{c29} (MVAR)	0.00	5	2.48706	2.36642	4.995	2.23148	2.32797	2.59549	0.955192	2.38303	1.48653	3.17221
Fuel cost ($/h)			**800.5099**	**646.8364**	**930.744**1	944.5003	967.6636	**859.1915**	**803.3125**	**801.2248**	**804.4838**	**830.639**
Emission(ton/h)			0.36645	0.28352	0.43493	**0.20482**	0.20727	0.22899	0.36344	0.36106	0.36127	0.25258
P_{Loss}(MW)			9.0345	6.8001	13.1378	3.2358	**3.1005**	**4.5404**	9.7206	8.9761	9.9486	**5.6219**
Q_{Loss}(MW)			39.614	29.6667	62.4263	22.6688	21.611	21.9075	42.6646	40.243	43.2192	27.2774
VD (p.u.)			0.90357	0.84479	0.44929	0.87393	0.88868	0.92852	**0.10842**	0.92655	0.91773	**0.29385**
L-index			0.13833	0.13867	0.15676	0.13888	0.13858	0.13814	0.14783	**0.13713**	**0.13917**	**0.14802**
P_{G1} (MW)	50	200	177.2131	139.9928	197.5689	64.9966	51.5005	102.8129	176.2053	175.6415	175.4861	121.9858

Table 5
Comparison of the MSA with MPSO, MDE, MFO and FPA for the single-objective OPF of IEEE 30 system.

Case #	Objective functions	MSA	MPSO	MDE	MFO	FPA
Case 1	Fuel cost ($/h)	**800.5099**	800.5164	800.8399	800.6863	802.7983
	Emission (ton/h)	0.36645	0.36624	0.3559	0.36849	0.35959
	P_{Loss}(MW)	9.0345	9.0354	8.8365	9.1492	9.5406
	Q_{Loss}(MW)	39.614	38.5749	39.2789	43.8331	44.942
	VD (p.u.)	0.90357	0.90488	0.77621	0.75768	0.36788
	L-index	0.13833	0.13825	0.14141	0.13914	0.14908
Case 2	Fuel cost ($/h)	646.8364	**646.7263**	650.2822	649.2727	651.3768
	Emission (ton/h)	0.28352	0.28349	0.28075	0.28336	0.28083
	P_{Loss}(MW)	6.8001	6.8008	6.9814	7.2293	7.2355
	Q_{Loss}(MW)	29.6667	28.9301	29.9268	40.3241	36.7308
	VD (p.u.)	0.84479	0.77475	0.57959	0.47024	0.31259
	L-index	0.13867	0.14004	0.13969	0.14269	0.14718
Case 3	Fuel cost ($/h)	930.7441	952.3039	930.9445	**930.7189**	931.7458
	Emission (ton/h)	0.43493	0.30123	0.43333	0.4352	0.43258
	P_{Loss}(MW)	13.1378	7.3049	12.7324	13.1787	12.1073
	Q_{Loss}(MW)	62.4263	30.9224	60.4379	63.7446	53.4394
	VD (p.u.)	0.44929	0.72294	0.44702	0.46718	0.46602
	L-index	0.15676	0.14028	0.15565	0.15693	0.15071
Case 4	Fuel cost ($/h)	944.5003	879.9464	927.8066	945.4553	948.949
	Emission (ton/h)	**0.20482**	0.23246	0.20926	0.20489	0.20523
	P_{Loss}(MW)	3.2358	7.0467	4.8539	3.4295	4.492
	Q_{Loss}(MW)	22.6688	35.2525	23.4377	17.8704	23.6465
	VD (p.u.)	0.87393	0.57387	0.39535	0.70968	0.42761
	L-index	0.13888	0.14294	0.1525	0.1393	0.14454
Case 5	Fuel cost ($/h)	967.6636	967.6523	967.6543	967.6785	967.1138
	Emission (ton/h)	0.20727	0.20727	0.20729	0.20727	0.20756
	P_{Loss}(MW)	**3.1005**	3.1031	3.1619	3.1111	3.5661
	Q_{Loss}(MW)	21.611	17.1822	19.1885	22.299	20.5784
	VD (p.u.)	0.88868	0.90632	0.76781	0.91558	0.3893
	L-index	0.13858	0.13816	0.14055	0.13815	0.14173

ferent cases have been provided to illustrate the effectiveness of the new approach for multi-objective problems. The results of the MSA algorithm are compared with those of MPSO, MDE, MFO, and FPA techniques, as given in Table 9. The weighted sum method is used to combine the objective functions of the OPF problem to construct a single objective function, as described in the following cases:

Case 6: minimization of fuel cost and active power losses

Table 6
Comparison of MSA and other algorithms reported in the literature for the single-objective OPF of IEEE 30 system.

Case #	Algorithm	Fuel cost ($/h)	Emission (ton/h)	P_{Loss}(MW)	Q_{Loss}(MW)	VD (p.u.)	L-index
Case 1	MSA	**800.5099**	0.36645	9.0345	39.614	0.90357	0.13833
	ARCBBO [2]	800.5159	0.3663	9.0255	NA	0.8867	0.1385
	RCBBO [2]	800.8703	NA	NA	NA	NA	NA
	GWO [3]	801.41	NA	9.30	38.58	NA	NA
	DE [3]	801.23	NA	9.22	38.91	NA	NA
	MGBICA [4]	801.1409	0.3296	NA	NA	NA	NA
	GBICA [4]	801.1513	0.3296	NA	NA	NA	NA
	ABC [5]	800.660	0.365141	9.0328	NA	0.9209	0.1381
	HSFLA-SA[19]	801.79					
Case 2	MSA	**646.8364**	0.28352	6.8001	29.6667	0.84479	0.13867
	LTLBO [9]	647.4315	0.2835	6.9347	NA	0.8896	NA
	TLBO [11]	647.9202	NA	7.1064	9.6327	1.4173	0.1211
	HMPSO-SFLA[17]	647.55	NA	NA	NA	NA	NA
	PSO[17]	649.41	NA	NA	NA	NA	NA
	GABC [20]	647.03	NA	6.8160	NA	0.8010	NA
Case 3	MSA	**930.7441**	0.43492	13.1358	62.4711	0.45435	0.15691
	ABC [5]	931.7450	NA	10.9570	NA	0.4575	NA
	GABC[20]	931.7450	NA	10.9570	NA	0.4575	NA
Case 4	MSA	944.3904	**0.20482**	3.2361	22.7432	0.88059	0.1387
	ARCBBO [2]	945.1597	0.2048	3.2624	NA	0.8647	0.1387
	MGBICA [4]	942.8401	0.2048	NA	NA	NA	NA
	GBICA [4]	944.6516	0.2049	NA	NA	NA	NA
	ABC [5]	944.4391	0.204826	3.2470	NA	0.8463	0.1402
	DSA [6]*	944.4086	0.2058255	3.24373	NA	NA	0.12734
	HMPSO-SFLA[17]	NA	0.2052	NA	NA	NA	NA
Case 5	MSA	967.6636	0.20727	**3.1005**	21.611	0.88868	0.13858
	ARCBBO [2]	967.6605	0.2073	3.1009	NA	0.8913	0.1386
	GWO [3]	968.38	NA	3.41	19.43	NA	NA
	DE [3]	968.23	NA	3.38	20.17	NA	NA
	ABC [5]	967.6810	0.207268	3.1078	NA	0.9008	0.1386
	DSA [6][a]	967.6493	0.20826	3.09450	NA	NA	0.12604
	EEA [7]	952.3785	NA	3.2823	NA	NA	NA
	EGA [7]	967.93	NA	3.244	NA	NA	NA
	ALC-PSO [8]	967.7683	NA	3.1700	NA	NA	NA

[a] The lower limit of load bus voltages is 0.9 p.u.

Table 7
Comparisons of average CPU simulation time for case 2 of IEEE 30 system.

Algorithm	Time (s)
MSA	14.91
MPSO	16.05
MDE	15.63
MFO	14.33
FPA	14.79
LTLBO [9]	22.78
MICA–TLA [21]	30.74
HMPSO-SFLA [17]	19.06

Table 8
Comparisons of the results obtained for case 2 of IEEE 30-bus system.

Algorithm	*Best*	*Average*	*Worst*
MSA	646.8364	646.8603	648.0322
MPSO	646.7263	649.8560	656.2251
MDE	650.2822	651.2573	653.3984
MFO	649.2727	649.8876	650.6213
FPA	651.3768	652.9572	654.3254
LTLBO [9]	647.4315	647.4725	647.8638
ABC [5]	649.0855	654.0784	659.7708
GABC [20]	647.03	647.0767	647.1234

This case is aimed to simultaneously minimize the fuel cost and the power transmission losses.The objective function can be expressed as follows:

$$f = \left(\sum_{i=1}^{NG} a_i P_{Gi}^2 + b_i P_{Gi} + c_i\right) + \lambda_P \sum_{i=1}^{nl} \sum_{j \neq i}^{nl} G_{ij} V_i^2 + V_j^2 - 2V_i V_j cos\left(\delta_i - \delta_j\right) + Penalty \quad (45)$$

Where, λ_P is a weighting factor, which is selected as 40.

Case 7: minimization of fuel cost and voltage deviation

The voltage profile is the most important index for system service quality. The improvement of the voltage profile contains reducing the deviation of load bus voltage from the unity. Considering only a cost-based objective function leads to a feasible solution with undesirable voltage deviations. Therefore, a multiple objective function is proposed to simultaneously minimize the fuel cost and voltage deviations (VD), which can be defined as follows:

$$f = \left(\sum_{i=1}^{NG} a_i P_{Gi}^2 + b_i P_{Gi} + c_i\right) + \lambda_{VD} \sum_{i=1}^{NL} |V_{L_i} - 1| + Penalty \quad (46)$$

Where, λ_{VD} is a weighting factor, which is selected in this case as 100.

Case 8: minimization of fuel cost with voltage stability enhancement The voltage stability is an important index for verification of power system ability to preserve constantly the voltage at each power system bus within suitable level under nominal operating conditions. A disturbance, change in system configuration, and rise in load demand are the main reasons for the voltage instability state in power system, which may lead to progressive decrease in voltage. Therefore, the minimization of voltage stability indicator, called L-index, is a significant objective function for power system planning and operation. The degree of voltage collapse of jth bus can be expressed, based on local indicators L_j, as follows:

$$L_j = |1 - \sum_{i=1}^{NG} F_{ji} \frac{V_i}{V_j}| \forall j = 1, 2, \ldots, NL \quad (47)$$

$$F_{ji} = -[Y_1]^{-1} [Y_2] \quad (48)$$

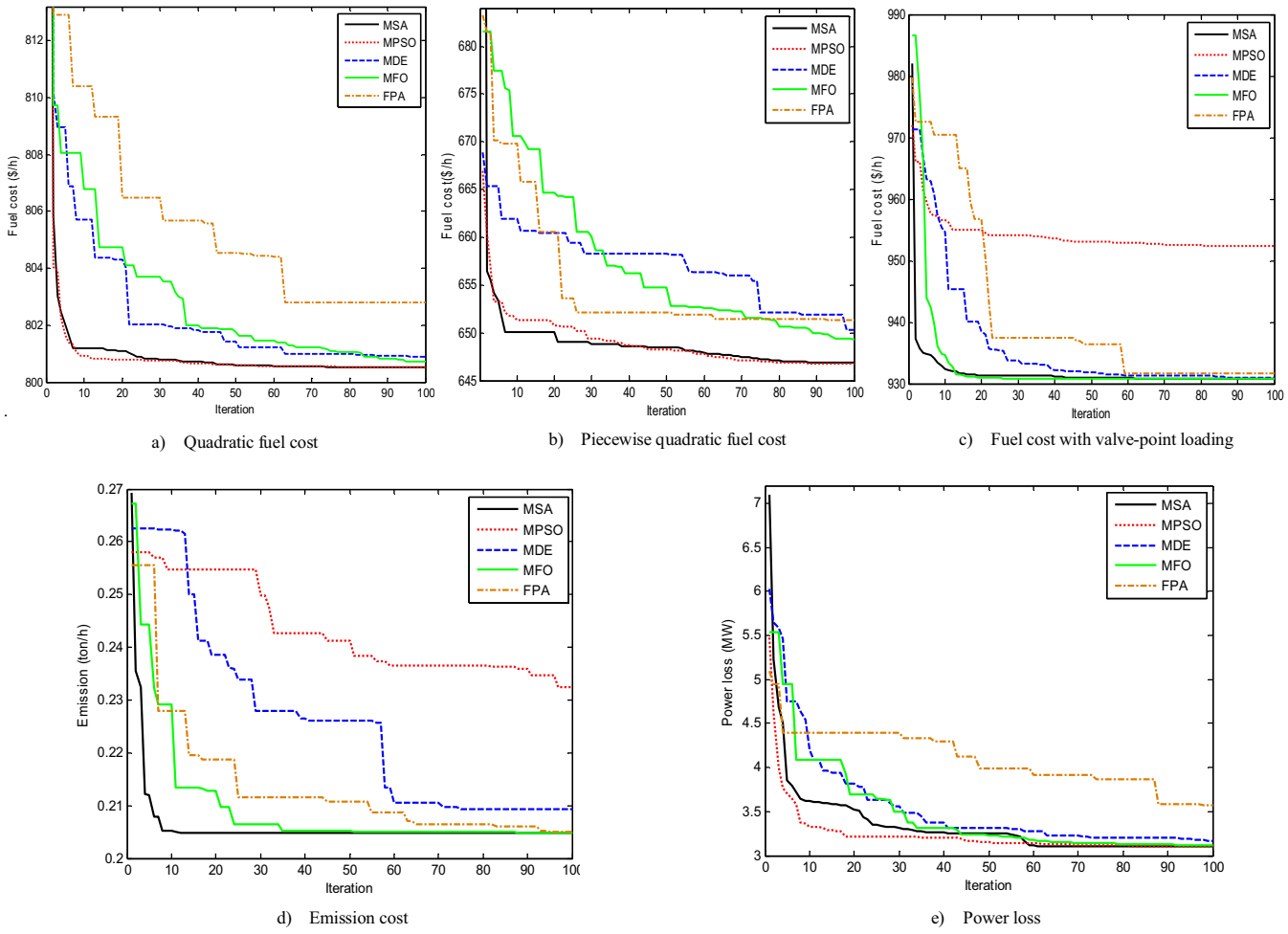

Fig. 3. Comparisons of convergence curves for single-objective OPF of IEEE 30 system.

Where, Y_1 and Y_2 are the system YBUS sub-matrices. The objective describing the system stability of complete system L-index can be expressed as follows:

$$L = max\left(L_j\right) \forall j = 1, 2, \ldots, NL \tag{49}$$

This case aims to optimize the quadratic fuel cost and in the same time keeps the system away from the voltage collapse point. Therefore, a twofold objective function is considered as follows:

$$f = (\sum_{i=1}^{NG} a_i P_{Gi}^2 + b_i P_{Gi} + c_i) + \lambda_L(max(L_j)) + Penalty \tag{50}$$

Where, the weighting factor λ_L, which is chosen as 100.

Case 9: minimization of fuel cost with voltage stability enhancement during contingency condition

The objective of this case is to minimize both the basic fuel cost and L-index using Eq. (50) and considering N-1 contingency simulated as outage of line (2–6). Whereas, the weighting factor λ_L, is taken as 200.

The convergence curves of the total cost (f) for all proposed optimizers are shown in Fig. 4.(a). It is quite obvious that the MSA has the best convergence characteristics. Variations of all components of total cost (i.e., fuel cost, voltage stability index and penalty function value) during iterations for MSA, MDE and FPA are shown in Fig. 4(b)–(d). We can notice from these figures that, penalty components are applied for each iteration of each method. In addition, these figures show the reduction in the penalty function value during the optimization process due to the acquisition of an adequate values for penalty terms, consequently guarantees a feasible solution without violations of constraints.

Case 10: minimization of cost, emission, voltage deviation, and losses

This case is aimed to simultaneously minimize four-conflicted objective of emission, losses, fuel cost and voltage deviations. Therefore, the objective function is to solve cases 4, 5 and 7 in the same time, which can be defined as follows:

$$f = \left(\sum_{i=1}^{NG} a_i P_{Gi}^2 + b_i P_{Gi} + c_i\right) + \lambda_E \left(\sum_{i=1}^{NG} \gamma_i P_{Gi}^2 + \beta_i P_{Gi} + \alpha_i + \zeta_i e^{(\lambda_i P_{Gi})}\right)$$
$$+\lambda_{VD}\left(\sum_{i=1}^{NL} |V_{L_i} - 1|\right) + \lambda_P \left(\sum_{i=1}^{nl}\sum_{j \neq i}^{nl} G_{ij}\left(V_i^2 + V_j^2 - 2V_iV_jcos(\delta_i - \delta_j)\right)\right)$$
$$+Penalty \tag{51}$$

Where, λ_E, λ_{VD}, and λ_P are the weighting factors, which are selected to balance between the objectives as 19, 21 and 22, respectively. This type of functions gives us a best visualization for the internal behaviour of the algorithms during the optimization process, which is appeared clearly in trajectories of the convergence for each component of the objective function, as given in Fig. 5. These convergence characteristics indicate that, the MPSO and MDE directed quickly towards their optimal values, which leads to premature convergence. The MFO and FPA indicated a severe changes along the search process, which leads to unstable final solution. In the

Table 9
Comparison of the MSA with MPSO, MDE, MFO and FPA for the multi-objective OPF of IEEE 30 system.

Case #	Objective functions	MSA	MPSO	MDE	MFO	FPA
Case 6	Fuel cost ($/h)	**859.1915**	859.5841	868.7138	858.5812	855.2706
	Emission (ton/h)	0.22899	0.2287	0.22525	0.22947	0.22959
	P_{Loss}(MW)	**4.5404**	4.5409	4.3891	4.5772	4.7981
	Q_{Loss}(MW)	21.9075	22.3987	24.2043	23.8781	24.5207
	VD (p.u.)	0.92852	0.94718	0.87816	0.89944	1.0143
	L-index	0.13814	0.13775	0.13787	0.13806	0.13811
	Total Cost	1040.808	1041.221	1044.054	1041.671	1055.719
Case 7	Fuel cost ($/h)	**803.3125**	803.9787	803.2122	803.7911	803.6638
	Emission (ton/h)	0.36344	0.3636	0.36218	0.36355	0.36803
	P_{Loss}(MW)	9.7206	9.9242	9.5974	9.8685	9.9252
	Q_{Loss}(MW)	42.6646	42.2652	40.867	50.6485	45.574
	VD (p.u.)	**0.10842**	0.1202	0.12646	0.10563	0.13659
	L-index	0.14783	0.14903	0.14943	0.14906	0.14751
	Total Cost	814.1545	815.9983	815.8582	814.3541	817.3228
Case 8	Fuel cost ($/h)	801.2248	801.6966	802.0991	801.668	**801.1487**
	Emission (ton/h)	0.36106	0.36194	0.35484	0.34299	0.3718
	P_{Loss}(MW)	8.9761	9.2003	9.0613	8.5578	9.3174
	Q_{Loss}(MW)	40.243	37.9253	37.2564	35.6815	39.4019
	VD (p.u.)	0.92655	0.83012	0.88754	0.83817	0.87563
	L-index	0.13713	0.13748	0.13744	0.13759	**0.13758**
	Total Cost	814.9378	815.4446	815.8431	815.4270	814.9067
Case 9	Fuel cost ($/h)	**804.4838**	807.6519	806.6668	804.556	805.5446
	Emission (ton/h)	0.36127	0.36043	0.37435	0.36078	0.36083
	P_{Loss}(MW)	9.9486	10.7581	10.7227	9.9532	10.1794
	Q_{Loss}(MW)	43.2192	49.5435	48.8165	42.2635	44.8919
	VD (p.u.)	0.91773	0.42848	0.56633	0.90195	0.4517
	L-index	**0.13917**	0.14051	0.13982	0.13935	0.14149
	Total Cost	832.3178	835.7539	834.6308	832.4266	833.8386
Case 10	Fuel cost ($/h)	**830.639**	833.6807	829.0942	830.9135	835.3699
	Emission (ton/h)	**0.25258**	0.25251	0.2575	0.25231	0.24781
	P_{Loss}(MW)	**5.6219**	6.5245	6.0569	5.5971	5.5153
	Q_{Loss}(MW)	27.2774	29.1151	28.4491	27.2355	26.6517
	VD (p.u.)	**0.29385**	0.18991	0.30347	0.33164	0.49969
	L-index	0.14802	0.14746	0.14872	0.14556	0.14873
	Total Cost	965.2905	986.0063	973.6116	965.8077	971.9076

Table 10
Optimal solutions obtained by MSA for IEEE 57 bus system.

variables	Min	Max	Case 11	Case 12	Case 13	variables	Min	Max	Case 11	Case 12	Case 13
P_{G2} (MW)	0.0	100	90.0784	85.34818	94.7494	T_{46} (PU)	0.90	1.10	0.9434363	0.9348021	0.904137
P_{G3} (MW)	0.0	140	45.186	45.85493	45.27931	T_{54} (PU)	0.90	1.10	0.9197841	0.900021	0.9823637
P_{G6} (MW)	0.0	100	68.98911	71.30797	65.03103	T_{58} (PU)	0.90	1.10	0.9930425	0.9479471	0.9823375
P_{G8} (MW)	0.0	550	462.8671	462.4092	460.1036	T_{59} (PU)	0.90	1.10	0.9893301	0.9608689	0.9692948
P_{G9} (MW)	0.0	100	94.13925	94.08068	97.86193	T_{65} (PU)	0.90	1.10	0.9889087	0.9781408	0.9783481
P_{G12} (MW)	0.0	410	361.2028	363.8543	360.2139	T_{66} (PU)	0.90	1.10	0.9543683	0.9182851	0.9564313
V_1 (PU)	0.95	1.10	1.065677	1.022121	1.069405	T_{71} (PU)	0.90	1.10	0.9730449	0.9509346	0.9661701
V_2 (PU)	0.95	1.10	1.063393	1.019646	1.067444	T_{73} (PU)	0.90	1.10	0.9659654	0.9941227	1.015854
V_3 (PU)	0.95	1.10	1.055744	1.013444	1.059587	T_{76} (PU)	0.90	1.10	0.9205493	0.9361633	1.036947
V_6 (PU)	0.95	1.10	1.059543	1.025691	1.062394	T_{80} (PU)	0.90	1.10	0.9977419	0.998129	1.011215
V_8 (PU)	0.95	1.10	1.071391	1.044968	1.076551	Q_{c18} (MVAR)	0.0	20.0	15.40877	11.88253	17.61211
V_9 (PU)	0.95	1.10	1.047925	1.014033	1.053227	Q_{c25} (MVAR)	0.0	20.0	16.56182	16.78665	8.381073
V_{12} (PU)	0.95	1.10	1.050537	1.010858	1.058035	Q_{c53} (MVAR)	0.0	20.0	16.40806	18.28455	8.796269
T_{19} (PU)	0.90	1.10	1.003475	0.9101725	0.9799597	Fuel cost ($/h)			**41673.7231**	**41714.9851**	**41675.9948**
T_{20} (PU)	0.90	1.10	1.008993	1.075124	1.042985	Emission (ton/h)			1.9526	1.9551	1.9188
T_{31} (PU)	0.90	1.10	0.9838953	0.9854176	1.032986	P_{Loss}(MW)			15.0526	15.9214	15.0026
T_{35} (PU)	0.90	1.10	1.007633	0.9872317	0.955761	Q_{Loss}(MW)			67.8569	75.2315	67.0164
T_{36} (PU)	0.90	1.10	1.015505	1.053424	1.021004	VD (p.u.)			1.5508	**0.67818**	1.7236
T_{37} (PU)	0.90	1.10	0.9981609	1.016568	1.028783	L-index			0.28392	0.29533	**0.27481**
T_{41} (PU)	0.90	1.10	0.9988305	1.00709	0.9928189	P_{G1} (MW)	0.0	575.88	143.3899	143.8661	142.5634

MSA, pathfinders and prospectors primarily carry out the exploration (global search), while onlookers and prospectors manage the exploitation (local search) ability of the proposed paradigm. Therefore, the MSA has some oscillations in the first iterations and settle down with the progress of the search process. Such a behaviour is a best guarantee to converge towards a final accurate solution [51].

4.2. IEEE 57-bus system

The IEEE 57-bus system [52] is considered to test the scalability of the proposed MSA algorithm. The system active and reactive power demand are 1250.8 MW and 336.4 MVAR, respectively. Three different objective functions are considered to illustrate the effectiveness of MSA for a relative large scale power system. A swarm of 100 moths with 14 pathfinders of MSA has been implemented to solve three objective functions of the OPF problem.

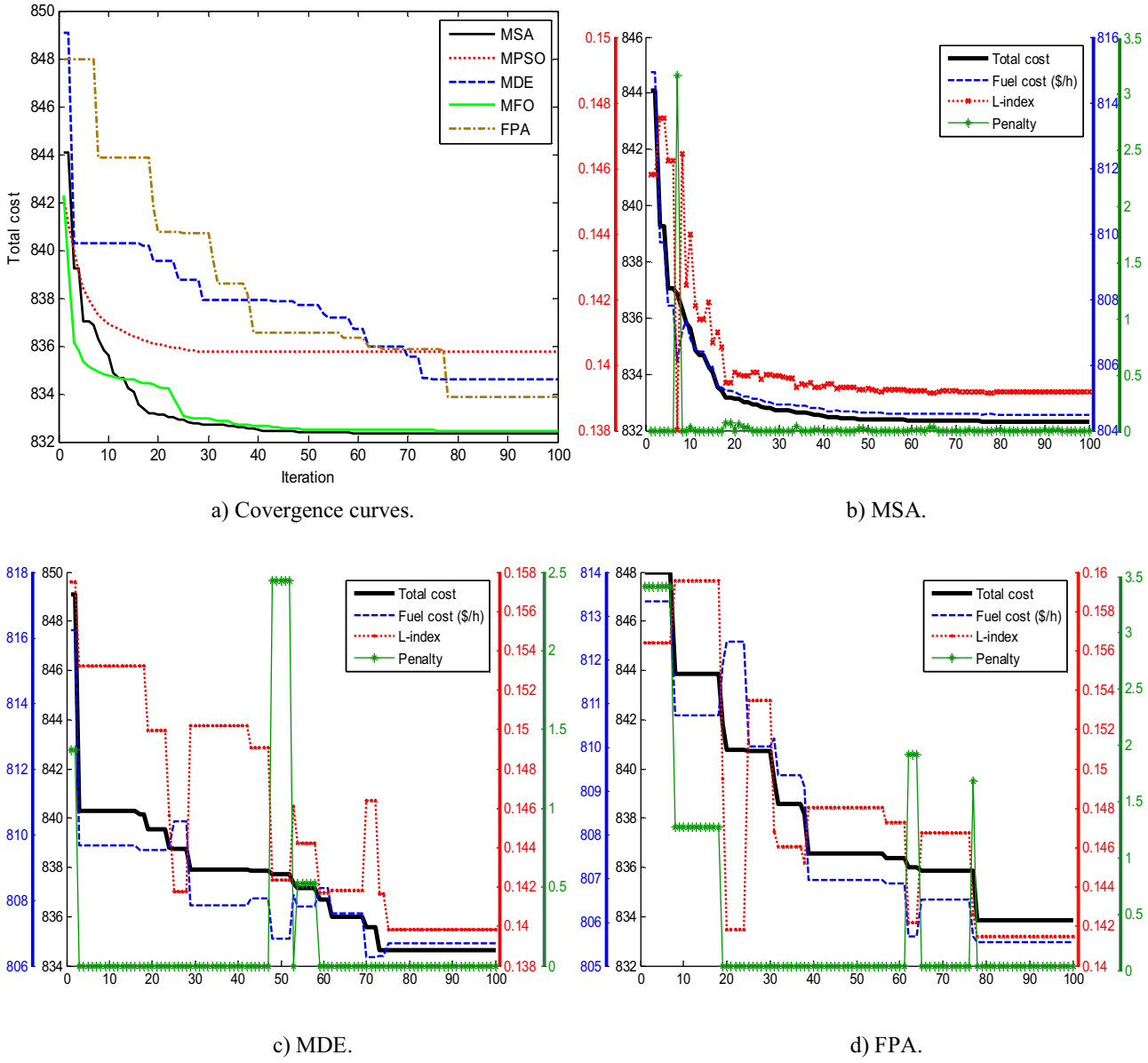

a) Covergence curves. b) MSA.

c) MDE. d) FPA.

Fig. 4. Covergence curves and variations of the components of total cost during iterations for case 9.

Table 11
comparison of the MSA with MPSO, MDE, MFO and FPA for IEEE 57 bus system.

Case #	Objective function	MSA	MPSO	MDE	MFO	FPA
Case 11	Fuel cost ($/h)	**41673.7231**	41678.6762	41695.8123	41686.4119	41701.9592
	Emission (ton/h)	1.9526	1.9443	2.0291	2.0036	2.0688
	P_{Loss}(MW)	15.0526	15.1271	15.9052	15.611	16.1543
	Q_{Loss}(MW)	67.8569	68.2332	71.3467	70.2146	71.4409
	VD (p.u.)	1.5508	1.3397	1.2101	1.2938	1.2818
	L-index	0.28392	0.28872	0.29232	0.29017	0.29183
Case 12	Fuel cost ($/h)	**41714.9851**	41721.6098	41717.3874	41718.8659	41726.3758
	Emission (ton/h)	1.9551	2.0096	1.9888	2.0149	1.9213
	P_{Loss}(MW)	15.9214	16.2453	16.0961	16.2189	16.027
	Q_{Loss}(MW)	75.2315	76.4918	76.0831	76.5491	74.6402
	VD (p.u.)	**0.67818**	0.67813	0.6781	0.67796	0.69723
	L-index	0.29533	0.2955	0.2952	0.29525	0.29488
	Total Cost	41782.8031	41789.4228	41785.1974	41786.6619	41796.0988
Case 13	Fuel cost ($/h)	**41675.9948**	41694.1407	41689.5878	41680.1937	41684.1859
	Emission (ton/h)	1.9188	1.977	2.0	1.9192	1.9223
	P_{Loss}(MW)	15.0026	15.4554	15.7092	15.1026	15.2193
	Q_{Loss}(MW)	67.0164	68.6211	70.6257	67.2447	67.7491
	VD (p.u.)	1.7236	1.5084	1.5447	1.7245	1.7478
	L-index	**0.27481**	0.27918	0.27677	0.27467	0.27429
	Total Cost	41703.4758	41722.0587	41717.2648	41711.6149	41707.6607

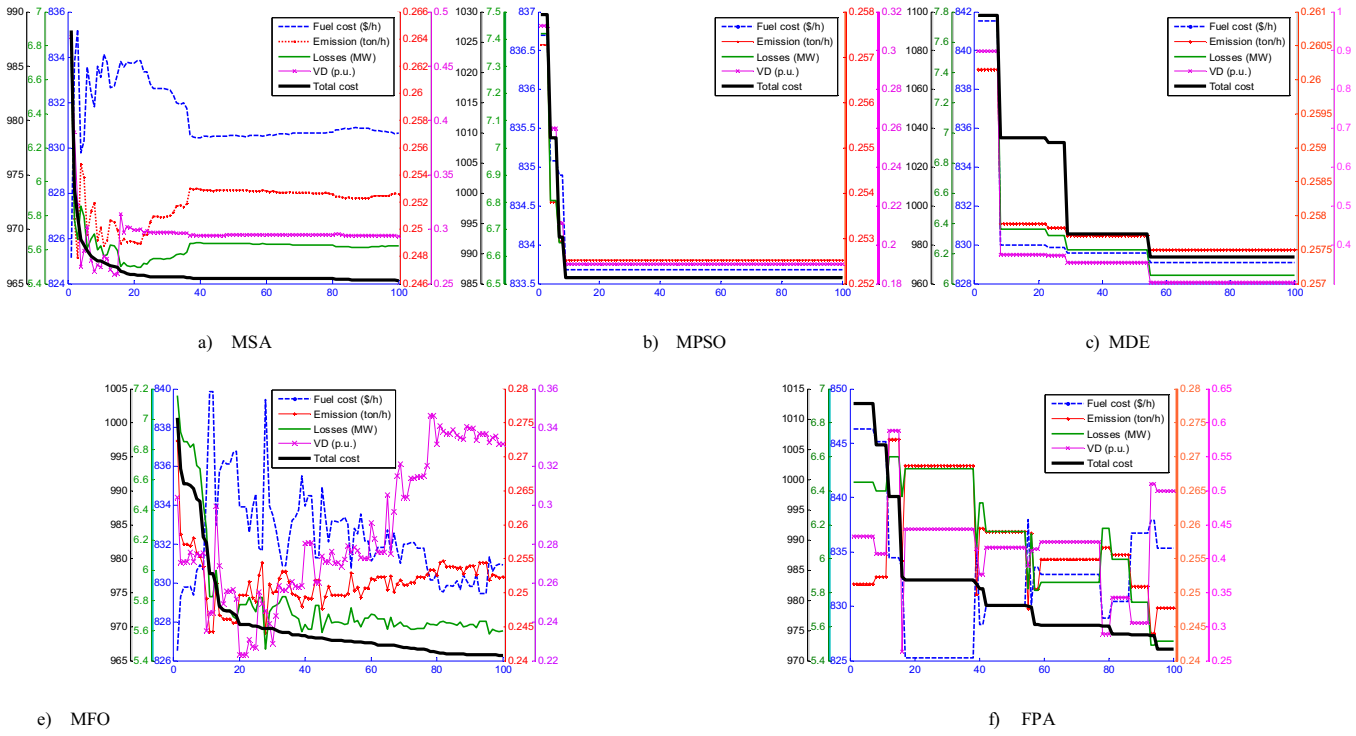

Fig. 5. Variations of the objective function components during iterations (case 10).

The control variables limits and the obtained optimzed settings of adjusting control parameters are given in Table 10. The MPSO, MDE, MFO, and FPA methods run also on all cases under the same conditions and population size. The comparative study of the final simulation results are tabulated in Table 11, shown that the MSA performed better than the rest of algorithms. Judging from Table 11, it can be seen that, the MSA method performed better than the other algorithms over all cases of IEEE 57-bus system.

Case 11: minimization of basic fuel cost

The objective function of this case is to optimize the fuel cost given by Eq. (38). The proposed MSA minimized the objective function, and provided remarkable results compared to those reported in the literature as given in Table 12.

Case 12: minimization of fuel cost and voltage deviation

In this case a multi-objective optimization, minimization of the fuel cost along with voltage profile enhancement, given by Eq. (46), where λ_{VD} is chosen as 100. It can be seen that the voltage magnitude deviations are greatly reduced and the total fuel cost is increased compared with case 11.

Case 13: minimization of fuel cost with voltage stability enhancement

The goal here is to minimize the fuel cost and at the same time to improve the voltage stability of the IEEE 57-test system. Thus, the objective function of Case 8 is given by Eq. (50) where λ_L is chosen as 100. It is clear that the value of L-index is reduced and the total fuel cost is slightly increased compared with case 11.

4.3. IEEE 118-bus system

A large-scale IEEE 118-bus system [52], is considered to further verify the effectiveness and the scalability of the proposed MSA algorithm. The system active and reactive power demand are 4242 MW and 1439 MVAR, respectively. All the algorithms introduced in 57-bus systems are used in this system with the same setting.

Case 14: minimization of basic fuel cost

Table 12
Comparison results of MSA and some other algorithms reported in the literature for case 11.

algorithm	Fuel cost ($/h)
MSA	**41673.7231**
KHA [10]	41 709.2647
LTLBO [9]	41679.5451
MGBICA [4]	41715.7101
GBICA [4]	41740.2884
ARCBBO [2]	41686
DSA [6]	41686.82
IEM [12][a]	4810.2161
MO-DEA [13]	41683
GSA[18]	41695.8717
ABC [5]	41693.9589
MICA–TLA [21]	41675.0545

[a] Limit of shunt VAR compensators is 5 MVAR.

As in cases 1 and 11, the objective function is to minimize the fuel cost given by Eq. (38). The best solution obtained using the proposed search algorithm are tabulated in Table 13. This result is compared to the four algorithms under study and some other techniques reported in the literature as given in Tables 14 and 15, respectively. It appears from these tables that, the MSA outperforms many optimization approaches used to solve OPF. Furthermore, the FPA obtains approciated results when deal with such large-scale system, which may explain the growing interest to include the Lévy-flights in a number of OPF solution methods.

4.4. Advantages of MSA

1 The procedure of fitness evaluation at the end of each phase and the dynamic change in population types provide a fast convergence rate, as shown in Fig. 3. From this figure, the MSA is a deep-PSO, fast-MFO and linear convergence characteristics of MDE and FPA.
2 The acquisition of different types of optimization strategies tends towards building a powerful algorithm, which has abil-

Table 13
Optimal solution obtained by MSA for IEEE 118 bus system.

Variables	Value	Variables	Value	Variables	Value	Variables	Value	Variables	Value
P_{G4}	0.7419968	P_{G65}	347.2867	P_{G116}	0	V_{G61}	1.061524	V_{G112}	1.02681
P_{G6}	2.33579	P_{G66}	344.9406	V_{G1}	1.03759	V_{G62}	1.056928	V_{G113}	1.051395
P_{G8}	0.766761	P_{G69}	663.6643	V_{G4}	1.058619	V_{G65}	1.062457	V_{G116}	1.056954
P_{G10}	394.8925	P_{G70}	3.687839	V_{G6}	1.050009	V_{G66}	1.073417	T_{8}	0.9886583
P_{G12}	85.69232	P_{G72}	2.906601	V_{G8}	1.041839	V_{G69}	1.086097	T_{32}	0.9964289
P_{G15}	17.62044	P_{G73}	2.832291	V_{G10}	1.051632	V_{G70}	1.061083	T_{36}	0.9847622
P_{G18}	33.77219	P_{G74}	20.51219	V_{G12}	1.045777	V_{G72}	1.054548	T_{51}	0.9786758
P_{G19}	32.41324	P_{G76}	18.22879	V_{G15}	1.044471	V_{G73}	1.058301	T_{93}	0.983802
P_{G24}	0.411386	P_{G77}	0.2434424	V_{G18}	1.045623	V_{G74}	1.049614	T_{95}	0.9981858
P_{G25}	190.7811	P_{G80}	423.527	V_{G19}	1.04533	V_{G76}	1.047129	T_{102}	1.029918
P_{G26}	273.6254	P_{G85}	0.3875764	V_{G24}	1.055204	V_{G77}	1.061483	T_{107}	0.9661403
P_{G27}	19.47055	P_{G87}	4.105519	V_{G25}	1.080674	V_{G80}	1.070869	T_{127}	0.9724915
P_{G31}	7.337286	P_{G89}	497.0322	V_{G26}	1.085966	V_{G85}	1.058588	Q_{c5}	24.03783
P_{G32}	28.63474	P_{G90}	2.061865	V_{G27}	1.048019	V_{G87}	1.048762	Q_{c34}	14.51845
P_{G34}	11.10953	P_{G91}	0.2893283	V_{G31}	1.039328	V_{G89}	1.074172	Q_{c37}	18.68108
P_{G36}	4.285056	P_{G92}	0.5276152	V_{G32}	1.045311	V_{G90}	1.056005	Q_{c44}	22.30433
P_{G40}	32.95023	P_{G99}	0.3722647	V_{G34}	1.053075	V_{G91}	1.059086	Q_{c45}	14.1212
P_{G42}	31.31559	P_{G100}	227.2744	V_{G36}	1.051457	V_{G92}	1.065375	Q_{c46}	24.63467
P_{G46}	19.51715	P_{G103}	37.82948	V_{G40}	1.041326	V_{G99}	1.058942	Q_{c48}	13.50065
P_{G49}	190.5231	P_{G104}	0.6184677	V_{G42}	1.043962	V_{G100}	1.061553	Q_{c74}	12.57651
P_{G54}	48.88164	P_{G105}	7.2594	V_{G46}	1.04981	V_{G103}	1.052396	Q_{c79}	7.944037
P_{G55}	36.84914	P_{G107}	34.48817	V_{G49}	1.062983	V_{G104}	1.043573	Q_{c82}	4.001553
P_{G56}	56.4017	P_{G110}	13.85596	V_{G54}	1.048727	V_{G105}	1.040572	Q_{c83}	7.929967
P_{G59}	146.1092	P_{G111}	35.63896	V_{G55}	1.048899	V_{G107}	1.033167	Q_{c105}	13.03137
P_{G61}	144.481	P_{G112}	29.2339	V_{G56}	1.048711	V_{G110}	1.036911	Q_{c107}	7.8869
P_{G62}	0	P_{G113}	1.414279	V_{G59}	1.060935	V_{G111}	1.041811	Q_{c110}	6.642801
							Fuel cost ($/h)		**129640.7191**
							P_{Loss}(MW)		73.2601
							Q_{Loss}(MW)		460.8088
							VD (p.u.)		3.0728
							L-index		0.061467
							P_{G1}(MW)		0

Table 14
comparison of the MSA with MPSO, MDE, MFO and FPA for IEEE 118 bus system.

Case #	Objective function	MSA	MPSO	MDE	MFO	FPA
Case **14**	Fuel cost ($/h)	**129640.7191**	132039.212	130444.5728	129708.0821	129688.7209
	P_{Loss}(MW)	73.2601	112.8486	71.6383	74.7063	74.3242
	Q_{Loss}(MW)	460.8088	718.2268	451.8952	469.639	467.4772
	VD (p.u.)	3.0728	1.1545	1.3146	2.3761	2.5391
	L-index	0.061467	0.068919	0.066577	0.062172	0.061775

ity to deal with the complex and multi-objective OPF problems, as clearly shown in Table 9.

3 Pathfinders have ability to implement the reconnaissance and scouting missions. Therefore, the proposed adaptive-crossover and lévy-mutation are able to zoom out the search space and support the exploration concept in large scale power systems of cases 11–14.

4 Lévy-flights stretch the searching process to discover a new areas, which is a best guarantee to bypass the stagnation situation. Therefore, the MSA has ability to avoid the premature convergence and withstand over the complicated boundaries in the problem of case 2.

5 The logarithmic spiral path as a relatively large scale non-linear updating mechanism has a great ability to deal with the valve-loading effects function in case 3.

6 Eq. (34) provides three advantages, which are: (a) Simulate the short-term memory of moth; (b) Address the problem of initial velocity in the basic PSO; (c) Reduce the required memory to store personal best solutions and velocities.

7 The sharing of information among the sub-swarms after each evaluation has an implicit form of memory, which can be considered as an inheritance memory, since it keeps track of the best solutions found during the optimization process. In addition, the harmony between the proposed updating equations provided the smooth convergence curve shown Fig. 4(b) and Fig. 5(a).

8 The following properties have been used to perform the time-saving in Table 7: (a) The dealing with each variable as an integrated unit; (b) Each one of updating methods is applied to a certain group of the population; (c) The associative learning mechanism reduces the required memory.

9 The dealing with a small number of best so far solutions divides the search space into smaller regions (subspace). This mechanism provides more effective search in lower dimensional space. Therefore, onlookers with their narrow scope exploitation help to make sure that the areas encircling the promising solutions does not contain any better alternative solutions and achieved final accurate solutions in Table 4.

10 The proposed dynamic flow of optimization process assists to strike a balance between exploration and exploitation and consequently helps for more scoping in the optimization space, which provided robust results for 30 trial run in Table 8.

11 The proposed adaptive crossover based on population diversity may be independently used for exploration-oriented hybridization to improve other local (neighborhood) search optimizers in the future. In addition, the mating between moths-genes in crossover operations in Eq. (25) obtained a new generation that has features from all best-so-far solutions. Meanwhile, the

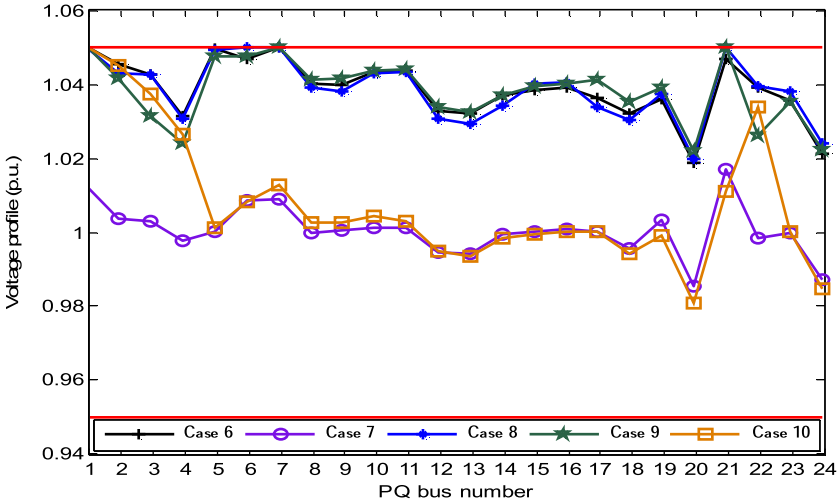

Fig. 6. Comparisons of the voltage profiles for the multi-objective cases of IEEE 30-bus system.

Table 15
Comparison results of proposed algorithm and other reported algorithms for IEEE 118 bus system.

Algorithm	Fuel cost ($/h)
MSA	**129640.7191**
TLBO [11]	129682.844
DSA [11]	129691.6152
FHSA [14]	132138.30
HSA [14]	132319.60
ICBO [15][a]	135121.5704
PSOGSA [16]	129 733.58

[a] Limit of shunt VAR compensators is 5 MVAR.

reliance on the population diversity in Eq. (26) achieves a scale-free operation.

4.5. Checking the feasibility

It is interesting to note that recently there some of published papers seem to have violated the limits of constraints, thereby yielding infeasible solutions. Infeasibility reasons of those papers implemented scrutinized extensively in Refs. [2,5,6,13,16,20]. These reasons summarized as inaccurate objective values, violations of the control-variables constraints and violations of the state-variables constraints.

In this study, the final solutions are tested after the optimization process to ascertain the accuracy. In addition, the control variables remained within their permissible limits, which can be seen in tabulated results obtained by the MSA. In addition, the state/dependent variables were obtained successfully by the proposed approach without any exceeding their limits using the penalizing strategy. As an example, the voltage magnitudes of all load buses that were achieved in the multi-objective cases of IEEE 30-bus system are shown in Fig. 6. This figure also illustrates that the voltage profiles in cases 7 and 10 are optimized compared with the other cases and more close to unity.

5. Conclusion

In this paper, a novel MSA paradigm has been presented and applied to solve several OPF objective functions in three test power systems. Four recently state-of-art evolutionary algorithms, namely MPSO, MDE, MFO and FPA, are implemented and compared with MSA, which can be considered a hybrid of those algorithms in line with the natural characteristics of the moth swarm. Further, new optimization operators have been proposed such as adaptive crossover based on population diversity and associative learning mechanism with immediate memory, which may be appropriate to hybrid with other algorithms in the future. From the obtained results, we can said that, the developed optimization algorithm is a deep-PSO, fast-MFO and linear convergence characteristics of MDE and FPA, and thus suitable for solving the non-smooth and complex problems. In addition, the comparative study with the proposed algorithms and published OPF solution methods confirms the primacy of the proposed paradigm and its potential to find valid and accurate solutions especially for multi-objective optimization problems and large-scale power systems.

References

[1] B. Xing, W.J. Gao, Introduction to Computational Intelligence InInnovative Computational Intelligence: A Rough Guide to 134 Clever Algorithms, 62, Springer International Publishing, 2014, pp. 3–17, http://dx.doi.org/10.1007/978-3-319-03404-11.
[2] A.R. Kumar, L. Premalatha, Optimal power flow for a deregulated power system using adaptive real coded biogeography-based optimization, Int. J. Electr. Power Energy Syst. 73 (2015) 393–399, http://dx.doi.org/10.1016/j.ijepes.2015.05.011.
[3] A.A. El-Fergany, H.M. Hasanien, Single and multi-objective optimal power flow using grey wolf optimizer and differential evolution algorithms, Electr. Power Compon. Syst. 43 (13) (2015) 1548–1559, http://dx.doi.org/10.1080/15325008.2015.1041625.
[4] M. Ghasemi, S. Ghavidel, M.M. Ghanbarian, M. Gitizadeh, Multi-objective optimal electric power planning in the power system using Gaussian bare-bones imperialist competitive algorithm, Inf. Sci. 294 (2015) 286–304, http://dx.doi.org/10.1016/j.ins.2014.09.051.
[5] M.R. Adaryani, A. Karami, Artificial bee colony algorithm for solving multi-objective optimal power flow problem, Int. J. Electr. Power Energy Syst. 53 (2013) 219–230, http://dx.doi.org/10.1016/j.ijepes.2013.04.021.
[6] K. Abaci, V. Yamacli, Differential search algorithm for solving multi-objective optimal power flow problem, Int. J. Electr. Power Energy Syst. 79 (2016) 1–10, http://dx.doi.org/10.1016/j.ijepes.2015.12.021.
[7] S.S. Reddy, P.R. Bijwe, A.R. Abhyankar, Faster evolutionary algorithm based optimal power flow using incremental variables, Int. J. Electr. Power Energy Syst. 54 (2014) 198–210. http://dx.doi.org/10.1016/j.ijepes.2013.07.019.
[8] R.P. Singh, V. Mukherjee, S.P. Ghoshal, Particle swarm optimization with an aging leader and challengers algorithm for the solution of optimal power flow problem, Appl. Soft Comput. 40 (2016) 161–177, http://dx.doi.org/10.1016/j.asoc.2015.11.027.
[9] M. Ghasemi, S. Ghavidel, M. Gitizadeh, E. Akbari, An improved teaching-learning-based optimization algorithm using Lévy mutation strategy for non-smooth optimal power flow, Int. J. Electr. Power Energy Syst. 65 (2015) 375–384, http://dx.doi.org/10.1016/j.ijepes.2014.10.027.
[10] P.K. Roy, C. Paul, Optimal power flow using krill herd algorithm, Int. Trans. Electr. Energy Syst. 25 (8) (2015) 1397–1419, http://dx.doi.org/10.1002/etep.1888.
[11] H.R.E.H. Bouchekara, M.A. Abido, M. Boucherma, Optimal power flow using teaching-learning-based optimization technique, Electr. Power Syst. Res. 114 (2014) 49–59. http://dx.doi.org/10.1016/j.epsr.2014.03.032.

[12] H.R. El-Hana Bouchekara, M.A. Abido, A.E. Chaib, Optimal power flow using an improved electromagnetism-like mechanism method, Electr. Power Compon. Syst. 8207 (2016) 1–16, http://dx.doi.org/10.1080/15325008.2015.1115919.
[13] A.M. Shaheen, R.A. El-Sehiemy, S.M. Farrag, Solving multi-objective optimal power flow problem via forced initialised differential evolution algorithm, IET Gener. Transm. Distrib. (2016), http://dx.doi.org/10.1049/iet-gtd.2015.0892.
[14] K. Pandiarajan, C.K. Babulal, Fuzzy harmony search algorithm based optimal power flow for power system security enhancement, Int. J. Electr. Power Energy Syst. 78 (2016) 72–79. http://dx.doi.org/10.1016/j.ijepes.2015.11.053.
[15] H.R.E.H. Bouchekara, A.E. Chaib, M.A. Abido, R.A. El-Sehiemy, Optimal power flow using an improved colliding bodies optimization algorithm, Appl. Soft Comput. 42 (2016) 119–131. http://dx.doi.org/10.1016/j.asoc.2016.01.041.
[16] J. Radosavljević, D. Klimenta, M. Jevtić, N. Arsić, Optimal power flow using a hybrid optimization algorithm of particle swarm optimization and gravitational search algorithm, Electr. Power Compon. Syst. 43 (17) (2015) 1958–1970, http://dx.doi.org/10.1080/15325008.2015.1061620.
[17] M.R. Narimani, R. Azizipanah-Abarghooee, B. Zoghdar-Moghadam-Shahrekohne, K. Gholami, A novel approach to multi-objective optimal power flow by a new hybrid optimization algorithm considering generator constraints and multi-fuel type, Energy 49 (2013) 119–136, http://dx.doi.org/10.1016/j.energy.2012.09.031.
[18] S. Duman, U. Güvenç, Y. Sönmez, N. Yörükeren, Optimal power flow using gravitational search algorithm, Energy Convers. Manage. 59 (2012) 86–95, http://dx.doi.org/10.1016/j.enconman.2012.02.024.
[19] T. Niknam, M.R. Narimani, R. Azizipanah-Abarghooee, A new hybrid algorithm for optimal power flow considering prohibited zones and valve point effect, Energy Convers. Manage. 58 (2012) 197–206, http://dx.doi.org/10.1016/j.enconman.2012.01.017.
[20] R. Roy, H.T. Jadhav, Optimal power flow solution of power system incorporating stochastic wind power using Gbest guided artificial bee colony algorithm, Int. J. Electr. Power Energy Syst. 64 (2015) 562–578, http://dx.doi.org/10.1016/j.ijepes.2014.07.010.
[21] M. Ghasemi, S. Ghavidel, S. Rahmani, A. Roosta, H. Falah, A novel hybrid algorithm of imperialist competitive algorithm and teaching learning algorithm for optimal power flow problem with non-smooth cost functions, Eng. Appl. Artif. Intell. 29 (2014) 54–69, http://dx.doi.org/10.1016/j.engappai.2013.11.003.
[22] I. BoussaïD, J. Lepagnot, P. Siarry, A survey on optimization metaheuristics, Inf. Sci. 237 (2013) 82–117, http://dx.doi.org/10.1016/j.ins.2013.02.041.
[23] A. Karami, A fuzzy anomaly detection system based on hybrid pso-kmeans algorithm in content-centric networks, Neurocomputing 149 (2015) 1253–1269, http://dx.doi.org/10.1016/j.neucom.2014.08.070.
[24] L. dos Santos Coelho, V.C. Mariani, J.V. Leite, Solution of Jiles-Atherton vector hysteresis parameters estimation by modified Differential Evolution approaches, Expert Syst. Appl. 39 (2) (2012) 2021–2025, http://dx.doi.org/10.1016/j.eswa.2011.08.035.
[25] D.H. Wolpert, W.G. Macready, No free lunch theorems for optimization, IEEE Trans. Evol. Comput. 1 (1) (1997) 67–82, http://dx.doi.org/10.1109/4235.585893.
[26] S.D. Müller, J. Marchetto, S. Airaghi, P. Koumoutsakos, Optimization based on bacterial chemotaxis, IEEE Trans. Evol. Comput. 6 (1) (2002) 16–29, http://dx.doi.org/10.1109/4235.985689.
[27] R. Rajabioun, Cuckoo optimization algorithm, Appl. Soft Comput. 11 (8) (2011) 5508–5518, http://dx.doi.org/10.1016/j.asoc.2011.05.008.
[28] A. Mutazono, M. Sugano, M. Murata, Energy efficient self-organizing control for wireless sensor networks inspired by calling behavior of frogs, Comput. Commun. 35 (6) (2012) 661–669, http://dx.doi.org/10.1016/j.comcom.2011.09.013.
[29] S. Mirjalili, Moth-flame optimization algorithm: a novel nature-inspired heuristic paradigm, Knowledge Based Syst. 89 (2015) 228–249, http://dx.doi.org/10.1016/j.knosys.2015.07.006.
[30] Xin-She Yang, Flower Pollination Algorithm for Global Optimization. In: Unconventional Computation and Natural Computation, Vol. 7445, Springer Lecture Notes in Computer Science, Berlin, Heidelberg, 2012, pp. 240–249, http://dx.doi.org/10.1007/978-3-642-32894-7_27.
[31] F. Tao, L. Zhang, Y. Laili, Improvement and Hybridization of Intelligent Optimization Algorithm In Configurable Intelligent Optimization Algorithm, 4, Springer International Publishing, 2015, pp. 107–126, http://dx.doi.org/10.1007/978-3-319-08840-24.
[32] G.G. Wang, A.H. Gandomi, A.H. Alavi, Stud krill herd algorithm, Neurocomputing 128 (2014) 363–370, http://dx.doi.org/10.1016/j.neucom.2013.08.031.
[33] S. Akpınar, G.M. Bayhan, A. Baykasoglu, Hybridizing ant colony optimization via genetic algorithm for mixed-model assembly line balancing problem with sequence dependent setup times between tasks, Appl. Soft Comput. 13 (1) (2013) 574–589, http://dx.doi.org/10.1016/j.asoc.2012.07.024.
[34] F. Zhao, Y. Hong, D. Yu, Y. Yang, Q. Zhang, A hybrid particle swarm optimisation algorithm and fuzzy logic for process planning and production scheduling integration in holonic manufacturing systems, Int. J. Comput. Integr. Manuf. 23 (1) (2010) 20–39, http://dx.doi.org/10.1080/09511920903207472.
[35] X. Wang, L. Gao, C. Zhang, X. Shao, A multi-objective genetic algorithm based on immune and entropy principle for flexible job-shop scheduling problem, Int. J. Adv. Manuf. Technol. 51 (5) (2010) 757–767, http://dx.doi.org/10.1007/s00170-010-2642-2.
[36] B. Mahdad, K. Srairi, Blackout risk prevention in a smart grid based flexible optimal strategy using Grey Wolf-pattern search algorithms, Energy Convers. Manage. 98 (2015) 411–429, http://dx.doi.org/10.1016/j.enconman.2015.04.005.
[37] K.D. Frank, Impact of outdoor lighting on moths: an assessment, J. Lepidopterists Soc. 42 (2) (1988) 63–93.
[38] K.J. Gaston, J. Bennie, T.W. Davies, J. Hopkins, The ecological impacts of nighttime light pollution: a mechanistic appraisal, Biol. Rev. 88 (4) (2013) 912–927, http://dx.doi.org/10.1111/brv.12036.
[39] F. Bartumeus, J. Catalan, U.L. Fulco, M.L. Lyra, G.M. Viswanathan, Optimizing the encounter rate in biological interactions: lévy vs. Brownian strategies, Phys. Rev. Lett. 88 (9) (2002) 097901–0979004, http://dx.doi.org/10.1103/PhysRevLett.88.097901.
[40] S. Borak, W. Härdle, R. Weron, Stable distributions Statistical Tools for Finance and Insurance, 2005, Springer, Berlin, Heidelberg, 2016, pp. 21–44, http://dx.doi.org/10.1007/3-540-27395-6.
[41] R.N. Mantegna, Fast, accurate algorithm for numerical simulation of Levy stable stochastic processes, Phys. Rev. E 49 (5) (1994) 4677–4683, http://dx.doi.org/10.1103/PhysRevE.49.4677.
[42] A. Mcfadyen, P. Corke, L. Mejias, Visual predictive control of spiral motion, IEEE Trans. Rob. 30 (6) (2014) 1441–1454, http://dx.doi.org/10.1109/TRO.2014.2361425.
[43] K.N. Boyadzhiev, Spirals and conchospirals in the flight of insects, Coll. Math. J. 30 (1999) 23–31.
[44] J.P. Cunningham, C.J. Moore, M.P. Zalucki, S.A. West, Learning, odour preference and flower foraging in moths, J. Exp. Biol. 207 (1) (2004) 87–94, http://dx.doi.org/10.1242/jeb.00733.
[45] R. Menzel, U. Greggers, M. Hammer, Functional Organisation of Appetitive Learning and Memory in a Generalist Pollinator, the Honey Bee. In Insect Learning: Ecological and Evolutionary Perspectives, in: A.C. Lewis (Ed.), Chapman and Hall, London, 1993, pp. 79–125, http://dx.doi.org/10.1007/978-1-4615-2814-2_4.
[46] R.J. Fan, Peter Anderson, B. Hansson, Behavioural analysis of olfactory conditioning in the moth Spodoptera littoralis (Boisd.)(Lepidoptera: noctuidae), J. Exp. Biol. 200 (23) (1997) 2969–2976.
[47] H.T. Skiri, M. Stranden, J.C. Sandoz, R. Menzel, H. Mustaparta, Associative learning of plant odorants activating the same or different receptor neurones in the moth Heliothis virescens, J. Exp. Biol. 208 (4) (2005) 787–796, http://dx.doi.org/10.1242/jeb.01431.
[48] O. Alsac, B. Scott, Optimal load flow with steady state security, IEEE Trans. Power Appl. Syst. 93 (3) (1974) 745–751, http://dx.doi.org/10.1109/TPAS.1974.293972.
[49] X. Yao, Y. Liu, G. Lin, Evolutionary programming made faster, IEEE Trans. Evol. Comput. 3 (2) (1999) 82–102, http://dx.doi.org/10.1109/4235.771163.
[50] X. Xia, A.M. Elaiw, Optimal dynamic economic dispatch of generation: a review, Electr. Power Syst. Res. 80 (8) (2010) 975–986, http://dx.doi.org/10.1016/j.epsr.2009.12.012.
[51] F. Van den Bergh, A.P. Engelbrecht, A study of particle swarm optimization particle trajectories, Inf. Sci. 176 (8) (2006) 937–971, http://dx.doi.org/10.1016/j.ins.2005.02.003.
[52] R.D. Zimmerman, C.E. Murillo-Sánchez, R.J. Thomas, Matpower (Available at:) http://www.pserc.cornell.edu/matpower.